



Exchange fluxes of CO₂, CH₄, N₂O and NO between soil and atmosphere along an ecoclimatic gradient in West African savannas: a missing piece for regional budgets

5 Moussa Zouré^{1,2}, Claire Delon², Adjon Kouassi¹, Dominique Serça², Corinne Galy-Lacaux², Sébastien Barot⁵, Money Osohou^{3,4}, Fulgence Koffi¹, Seydina Mohamad Ba⁹, Adeola Michael Dahunsi², Xavier Le Roux⁶, Silué Siélé⁷, Ousmane Ndiaye⁸, Océane Lenoir², Eric Gardrat², Maria Dias-Alves², Sarah Konaré⁷, Madina Doumbia⁷, Fabien Solmon^{2,11}, Hagninou Elagnon Venance Donnou¹⁰

10 ¹Laboratoire des Sciences et Techniques de l'Environnement, Université Jean Lorougnon Guédé, Daloa, Côte d'Ivoire

²Laboratoire d'Aérodologie, Université de Toulouse, CNRS, IRD, LAERO, Toulouse, France

³Département de Physique, Université de Man, Man, Côte d'Ivoire

⁴Laboratoire des Sciences de la Matière, de l'Environnement et de l'Energie Solaire (LASMES), Université Félix-Houphouët Boigny (UFHB), Abidjan, Côte d'Ivoire

15 ⁵IRD, Sorbonne Université, CNRS, INRAE, Université Paris Diderot, UPEC, UMR 7618, Institute of Ecology and Environmental Sciences – Paris, France

⁶INRAE, CNRS, Université de Lyon, Laboratoire d'Ecologie Microbienne, Lyon, France

⁷Université Péléforo Gon Coulibaly de Korhogo, Unité de Formation et de Recherche des Sciences Biologiques, Korhogo, Cote d'Ivoire

20 ⁸Institut Sénégalais de Recherches Agricoles, Centre de Recherche Zootechniques, Dahra, Sénégal

⁹Faculté des Sciences et Techniques (FST), Institut des Sciences de l'Environnement (ISE), Université Cheikh Anta Diop (UCAD) de Dakar, Sénégal

¹⁰Laboratoire de Sciences des Matériaux et Modélisation (LaSMMo), Faculté des Sciences et Techniques, Université d'Abomey-Calavi, Cotonou, Benin

25 ¹¹Institute for Atmospheric and Climate Science, ETH Zurich, Switzerland

Correspondence to: Moussa Zouré (moussa.zoure@utoulouse.fr) and Claire Delon (claire.delon@cnrs.fr)

Abstract

30 This study investigated greenhouse gas (CO₂, CH₄, N₂O) and reactive nitrogen (NO) fluxes at three West African savanna sites: the international research reserve of Lamto (Taabo district, Côte d'Ivoire), the Observatoire de Recherche en Environnement de Nambekaha (OREN) (Korhogo, Côte d'Ivoire), and the Centre de Recherches Zootechniques (Dahra, Senegal). Measurements were carried out during intensive field campaigns conducted in 2024 and 2025, during the wet seasons at the three sites, across tree areas and grassy areas in savannas, and
35 cropland ecosystems subjected to different treatments from March 2023 to September 2025.

Overall, soil moisture, vegetation type (grassy areas, trees areas, crops) and site location (Lamto, Dahra, Nambekaha) were the main factors controlling gas fluxes (CO₂, NO and CH₄), whereas treatments containing different ratio of nitrates and ammonium had no significant effect according to the statistical analysis (ANCOVA).



40 CO₂ fluxes ranged from 8.21 ± 2.5 to 91.35 ± 73.2 $\mu\text{g C m}^{-2} \text{ s}^{-1}$ and were controlled by soil
moisture, with a decrease in soil respiration as water content increased ($\beta = -1.105 \pm 0.236$ μg
C $\text{m}^{-2} \text{ s}^{-1}$; $p < 0.001$), due to a limitation of oxygen diffusion in the soil, highlighting the key
role of soil moisture in regulating both heterotrophic microbial respiration and autotrophic plant
respiration, in relation to soil aeration conditions. NO emissions, ranging from 0.01 ± 0.0 to
45 497.39 ± 146.3 $\text{ng N m}^{-2} \text{ s}^{-1}$, showed a significant correlation with vegetation type. The highest
values were observed in the cropland plots of Nambekaha ($\beta = +76.779 \pm 15.82$ $\text{ng N m}^{-2} \text{ s}^{-1}$;
 $p < 0.001$) compared with natural savannas, reflecting intensified nitrification processes linked
to background fertilization inputs ($150 \text{ kg NPK ha}^{-1} \text{ yr}^{-1}$).

CH₄ fluxes were primarily determined by vegetation type: grassy areas within savannas
50 behaved as net sources ($\beta = +3.836 \pm 0.62$; $p < 0.0001$), whereas croplands acted as sinks,
suggesting methanotrophic activity capable of oxidizing atmospheric methane in the soil. In
contrast, N₂O fluxes were mostly low or even negative across all ecosystems and treatments,
with no significant relationship to soil moisture, vegetation type, or treatments. The results
indicate that soils could occasionally function as net N₂O sinks: indeed, N₂O uptake may occur
55 in nitrogen-poor soils under oxic conditions where the limited availability of mineral nitrogen
restricts N₂O production and where atmospheric N₂O diffuses easily into the soil.

These findings highlight the microbial and environmental coupling of carbon and nitrogen
dynamics in tropical savanna soils and provide critical insight for predicting greenhouse gas
and reactive gas emissions under changing land-use conditions.

60 **Keywords:** greenhouse gas; reactive nitrogen; biogeochemical cycles; soil moisture; vegetation
type; West Africa, emissions; soil processes.

65

70



1. Introduction

75 Greenhouse gases (GHGs) emission increase is today among the main drivers of global climate change. They play a central role because of their combined contribution to radiative forcing and their involvement in terrestrial and atmospheric feedbacks (World Meteorological Organization, 2022; IPCC, 2021; Ravishankara et al., 2009; Tian et al., 2020). In parallel, short-lived nitrogen oxides (NO) strongly influence the formation of tropospheric ozone, a secondary pollutant with major health and climate impacts (Fadnavis et al., 2025).

80 CO₂ fluxes from soils are mainly driven by autotrophic and heterotrophic respiration, whereas CH₄ fluxes are largely controlled by microbial methane oxidation in soils. N₂O and NO fluxes mainly result from nitrification and denitrification processes. These greenhouse gas and reactive compound fluxes are highly sensitive to environmental factors such as soil moisture and temperature, mineral nitrogen availability, soil structure and organic matter content (Bratti et al., 2022; Davidson and Verchot, 2000; Liu et al., 2022; Robertson et al., 2000, Butterbach-Bahl et al., 2013; Lu et al., 2022; Syakila and Kroeze, 2011).

Tropical regions, especially in Africa, play a decisive role in these dynamics. They host a wide diversity of soils and ecosystems, ranging from humid forests to dry savannas, including croplands and fallows. Yet, despite their ecological and climatic importance, these regions remain among the least documented in the world regarding GHGs and reactive nitrogen fluxes (Daelman et al., 2025; Reay et al., 2012; Stehfest and Bouwman, 2006). West Africa in particular is dominated by savanna ecosystems that cover vast areas and exhibit strong climatic gradients from south to north. These savannas, subjected to a strong alternation between dry and wet seasons, constitute ideal environments for studying pulsed emissions, particularly for 95 CO₂, N₂O and NO.

The few studies previously conducted in West Africa reveal considerable heterogeneity in N₂O and NO fluxes, reflecting strong gradients in soil texture, organic matter content, agricultural practices, atmospheric deposition, and moisture conditions (Delon et al., 2010; Serça et al., 1998). The distribution of vegetation is driven by the precipitation gradient and influences N and C fluxes between the soil and the atmosphere through decomposition and quality of organic matter (Parton et al., 2007), absorption of mineral N by growing plants (Potter et al., 1996), inhibition of nitrification by specific grasses, and stimulation by trees (Srikanthasamy et al., 2018). Each system encompasses specific processes in driving the N and C cycles in the soil, combined to environmental and climatic conditions. Therefore, the study of N and C cycles in one specific site needs to include the comparison of soil processes in each area, *i.e.* grass and tree areas. In addition, to cover a broader range of systems, it is necessary to incorporate studies of processes in crops in order to understand the disturbance of biogeochemical cycles caused by human activity.

110 Although soils are most often considered as sources of N₂O, recent studies in tropical regions indicate that they can also function as temporary, or even net, sinks (Chapuis-Lardy et al., 2007; Gallarotti et al., 2021). By contrast, upland soils are generally considered as sinks of CH₄ because atmospheric methane is oxidized by methanotrophic microorganisms under well



aerated conditions, whereas water saturated and oxygen limited soil can become source of CH₄ (Lim et al., 2024; Song et al., 2024). Whether soils act as net sources or net sinks of greenhouse
115 gases largely depends on soil moisture conditions, soil aeration status, mineral nitrogen availability, and microbial activity (H. Liu, Li, et al., 2022; H. Liu, Zheng, et al., 2022). Rewetting pulses, initiated by the first rains following a dry period, are particularly well documented as moments of high N₂O and NO release (Krichels et al., 2022; Leitner et al., 2017; Leitner et al., 2024; Yagle and Gelfand, 2025). Despite these pioneering contributions, it
120 remains difficult to generalize the biogeochemical behavior of rural tropical soils due to the lack of long-term measurements and the absence of datasets covering broad climatic gradients.

Atmospheric nitrogen deposition is another key factor capable of altering gaseous emission dynamics. Since the industrial era, reactive nitrogen deposition has increased markedly worldwide as a result of agriculture, industrialization, and traffic, with emerging hotspots in
125 developing countries at low latitudes, including West Africa (Lamarque et al., 2013; Ossohou et al., 2021; Vet et al., 2014). Increased nitrogen deposition can stimulate soil N compound emissions at the global scale, as shown by recent syntheses directly linking nitrogen inputs to enhanced N₂O fluxes (Cen et al., 2024). In African savannas, where soils are often nutrient-limited, even small increases in available nitrogen can trigger strong responses. Furthermore,
130 the partition of deposited nitrates vs ammonium by rain is an important information as each compound will not have the same effect on soil processes (and subsequent emissions to the atmosphere). Both nitrogen species deposition might not be impacted the same way by anthropogenic activity in the future.

Given these elements, understanding GHGs and reactive nitrogen fluxes from tropical soils is
135 essential for improving regional and global emission budgets as well as for refining biogeochemical and climate models. Indeed, most current models face large uncertainties when simulating emissions in tropical regions due to the scarcity of local data (Song et al., 2024; Van Lent et al., 2015; W. Wang et al., 2013), particularly in rural areas. These uncertainties are further amplified in dry and semi-arid environments, where the limited number of field
140 measurements and the strong nonlinearity of biogeochemical processes complicate the parameterization of emissions.

The present study is part of the NitroAfrica project which aims to understand the impact of wet nitrogen deposition on soil processes, vegetation, and fluxes to the atmosphere. Within the NitroAfrica framework, this study is more specifically interested in investigating gas exchanges
145 between soils and the atmosphere and to assess the impact of wet nitrogen deposition on these fluxes. It aims to quantify, compare, and analyze CO₂, CH₄, N₂O, and NO fluxes at three rural sites in West Africa spanning a broad ecoclimatic gradient from humid to semi-arid savannas: Lamto (Côte d'Ivoire) represents a humid savanna (Konan et al., 2021), Dahra (Senegal) a Sahelian arid savanna (Laouali et al., 2021) and Nambekaha (Côte d'Ivoire) a Sudanian savanna.

This south–north gradient provides an ideal framework for investigating how climatic, edaphic,
150 and atmospheric factors modulate soil–atmosphere trace gas exchanges. Measurements conducted in 2024–2025 made it possible to compare fluxes across the three sites, and to assess



if CO₂, CH₄, N₂O and NO exchanges show similarities or differences with patterns usually highlighted in equivalent ecosystems.

- 155 Several questions will be raised in this study: (i) does the response of fluxes depend on vegetation type (tree vs grass vs crops)? (ii) how are the fluxes influenced by the precipitation regime (less intense fluxes in drier areas)? (iii) does the partition in nitrates and ammonium in wet deposition influence the gas exchanges? Answering those questions in this study will help in (1) better characterizing natural GHGs and NO soil-atmosphere exchanges in tropical rural zones in Sub Saharan Africa (SSA); (2) evaluating the influence of atmospheric nitrogen deposition and moisture variability on fluxes to the atmosphere; (3) determining the rank of importance in influencing variables (nitrogen deposition, soil moisture, vegetation type, sites) on gas exchanges between the soil and the atmosphere.
- 160

2. Materials and Methods

165 2.1. Study Sites

The study was conducted at three contrasting sites located along a south–north climatic gradient in West Africa: Lamto, Nambekaha, and Dahra (Fig 1). These sites represent ecological zones ranging from humid savanna to Sahelian savanna from South to North, providing an ideal framework for studying the variability of greenhouse gas and reactive nitrogen exchanges between the soil and the atmosphere.

170

- **Lamto (Côte d’Ivoire, 6°13’N, 5°02’W)**

The Lamto site is located in Côte d’Ivoire, within the Taabo district, approximately 120 km northwest of Abidjan, along the banks of the Bandama River, and covers an area of about 2617 ha. It is situated at about 6°13’ N latitude and 5°02’ W longitude. Lamto is an international scientific research platform constituted by two stations, the ecological station supervised by the Centre de Recherche en Ecologie from University Nangui Abrogoua, and the geophysical station supervised by the Laboratoire des Sciences de la Matière, Environnement et Energie Solaire (LASMES), Félix Houphouët-Boigny University.

175

The ecological research station is dedicated to the study of savanna ecosystems, with the main objectives of understanding the structure, functioning, and dynamics of tropical savannas, including interactions between vegetation, soils, and climate. Studies conducted there are interesting in investigating the biogeochemical cycles of carbon and nitrogen and the processes controlling greenhouse gas exchanges between soils, vegetation, and the atmosphere, and producing long-term datasets (Abbadie et al., 2006; Tiemoko et al., 2020). The geophysical station focused on climate change through continuous measurements of meteorological parameters and atmospheric chemical composition, in order to better understand local and regional atmospheric processes and their interactions with ecosystems and rural environments (Diawara et al., 2014; Ossouhou et al., 2021; Tiemoko et al., 2023).

180

185

Mean annual rainfall amounted to 1090.9 mm in 2018, 1508.2 mm in 2019, and 1101.4 mm in 2020, yielding an average of 1233.5 ± 238 mm (Diaby et al., 2023). The wet season extends

190



from April to October and the dry season from November to March. The rainfall profile at Lamto is bimodal, with maximum rainfall in June and October. Vegetation is dominated by grasses, mainly *Hyparrhenia diplandra* (Koffi et al., 2019; Srikanthasamy et al., 2018), forming a mosaic of grassy areas and trees areas in savannas, and gallery forests along watercourses. It is typical of the forest–savanna transition zone at the tip of the “V-Baoulé” in Côte d’Ivoire. Soils are hydromorphic ferruginous soils, composed of approximately 77% sand, 14% silt, and 9% clay (Srikanthasamy et al., 2018). Soil pH measurements conducted during the field campaigns revealed slightly basic soils, with a mean pH of 7.24 ± 0.07

- **Nambekaha (Côte d’Ivoire, 9°18’N, 5°43’O)**

The Nambekaha study site was selected for the establishment of the Observatoire de Recherche en Environnement de Nambekaha (OREN), under the coordination of Peleforo Gon Coulibaly University (UPGC, Korhogo). Mean annual rainfall in Korhogo (25 km away from Nambekaha) was 1160.1 mm in 2018, 1162.5 mm in 2019, and 1083 mm in 2020 (average 1135.2 ± 45.2 mm, Diaby et al., 2023). Korhogo is characterized by a unimodal rainfall regime with a single wet season from April to October and a single dry season from November to March (Diaby et al., 2023). OREN is an interdisciplinary scientific infrastructure dedicated to the study of environmental dynamics, including climate, hydrology, biodiversity, soils, and agricultural activities. The area represents a hotspot for the expansion of cotton, rice, and cashew cultivation, all of those crops relying on fertilizer inputs for production (Diaby et al., 2023). Soil pH measurements conducted during the NitroAfrica field campaigns revealed slightly acidic soils, with a mean pH of 6.78 ± 0.08 . To date, no detailed study has yet been published on the physico-chemical of soils characteristics and the vegetation type at the OREN site, representing a significant gap in our understanding of this ecosystem. In addition, the agricultural site of Nambekaha received $150 \text{ kg NPK ha}^{-1} \text{ yr}^{-1}$ fertilizer inputs in 2024 before our field campaign.

- **Dahra (Senegal, 15°24’N, 15°26’W)**

The Dahra study site is located in the Sahelian sylvopastoral zone of northwestern Senegal, within the Centre de Recherches Zootechniques (CRZ), an experimental station operated by the Institut Senegalais de Recherche Agricole (ISRA) ($15^{\circ}24'10'' \text{ N}$, $15^{\circ}25'56'' \text{ W}$). The CRZ of Dahra is one of the major Sahelian research sites dedicated to the study of pastoral systems, savanna dynamics, and soil–vegetation–livestock interactions (Tagesson et al., 2015).

The climate is Sahelian, characterized by a unimodal rainfall pattern. The rainy season lasts on average about 3 to 4 months from July to October. Between 2012 and 2020, the site recorded an average annual rainfall of 380 mm, with strong interannual variability (271–529 mm, Delon et al., 2022). Mean annual temperature is around $28.9 \text{ }^{\circ}\text{C}$ (Sene et al., 2017).

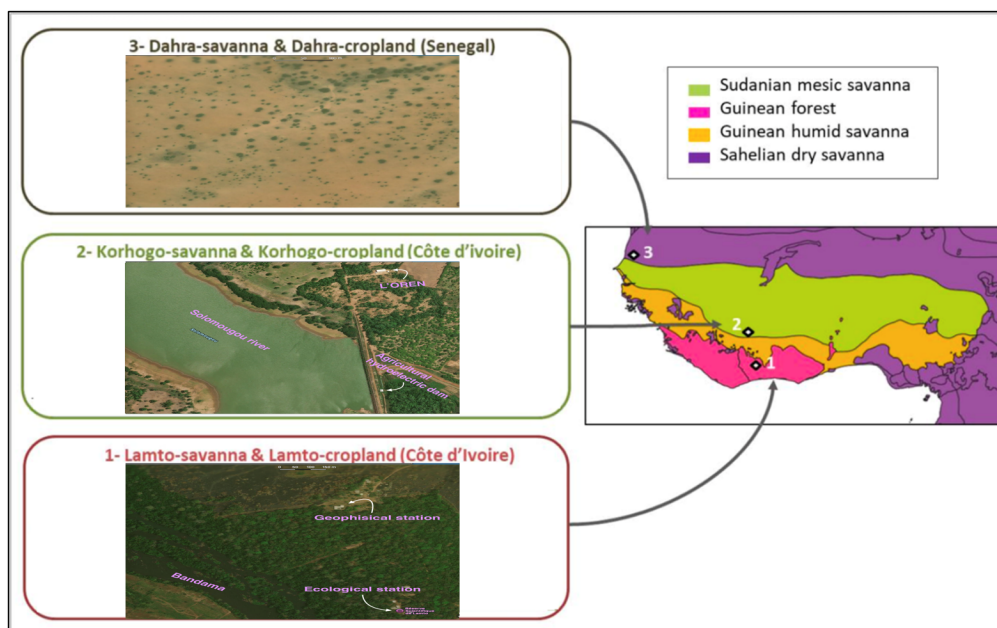
Soils at the CRZ of Dahra have a high sandy texture, consisting of approximately 89% sand and 6.3% clay. In the 0–5 cm surface layer, soil pH ranges from 6.2 to 7.4, indicating an overall neutral but spatially heterogeneous soil environment (Delon et al., 2022).

Tree cover at the CRZ is low, ranging from 3% (Rasmussen et al., 2011) to 6.4% (Tagesson et al., 2015). Dominant tree species include *Acacia raddiana*, *Balanites aegyptiaca*, *Acacia*



230 *senegal*, *Acacia tortilis*, and *Leptadenia hastata*. The herbaceous layer is dominated by grasses
 such as *Dactyloctenium aegyptium*, *Aristida adscensionis*, *Cenchrus biflorus*, *Eragrostis*
tremula and *diodela sarmentosa*. These grasses, adapted to short wet-dry cycles, provide most
 of the forage resource during the growing season (Miehe et al., 2010).

235 The CRZ of Dahra operates as an open sylvopastoral system where grazing occurs permanently
 throughout the year. The livestock includes mainly cattle, sheep, and goats. Grazing pressure is
 estimated between 242 and 1210 animals over approximately 500 ha, nearly four times the
 regional average (Agbohessou et al., 2024).



240 Figure 1: Locations of the three measurement sites on the Nambekaha (Korhogo)-Lamto-Dahra transect :
 (1) map of Lamto vegetation in Côte d'Ivoire, (2) map of Nambekaha (Korhogo) vegetation in Côte
 d'Ivoire and (3) map of Dahra vegetation in Sénégal. The ecoclimatic base map was provided by the
 NitroAfrica project team. The ecoclimatic background map was provided by the NitroAfrica project
 team (credit: NitroAfrica project). Site location panels are based on satellite imagery from Apple Maps
 (© Apple / TomTom / Maxar, as applicable) and were annotated by the authors.

245 2.2. Experimental Design

Atmospheric nitrogen (N) deposition is increasingly recognized as a major global change driver
 affecting tropical ecosystems (Lamarque et al., 2013; Matson et al., 1999; Zhang et al., 2021).
 At the Lamto site (Côte d'Ivoire), Ossohou et al. (2021) reported a significant increase in wet
 nitrogen deposition over the period 1994-2015 with the annual rise of +3.25% yr⁻¹. Wet
 250 deposition represents the dominant component of total atmospheric nitrogen deposition (wet +
 dry) at Lamto, accounting for approximately 70% of total N deposition. At a broader scale,
 projections suggest that N deposition to ecosystems, particularly in wet form, could increase by
 nearly 50% by 2100 (Lamarque et al., 2013).



In this context, a 2.5 years field experiment was conducted at the three sites (Lamto, Nambekaha, Dahra), to investigate the effect of different ratios of oxidized (nitrates, NO_3^-) and reduced (ammonium, NH_4^+) N deposition. The study focused on three major ecosystem types at each site: grass-dominated areas, tree-dominated areas, and cultivated fields. Crop types differed according to site and year to reflect local agricultural practices. At Lamto, experiments were conducted in maize fields during the 2024 and 2025 growing seasons. At Nambekaha, cotton was cultivated in 2024 and rice in 2025, whereas at Dahra, peanut crops were studied in 2024 and bean crops in 2025.

In the following, results will be presented referring to grass area, trees and crops. Each ecosystem type consisted of 16 experimental plots corresponding to four treatments with four replicates per treatment. Consequently, a total of 48 plots were established per site. Individual plots measured $2.5 \text{ m} \times 2.5 \text{ m}$ (6.25 m^2) and were separated from one another to minimize lateral transfer and cross contamination between treatments.

Four types of solutions corresponding to distinct nitrogen treatments were prepared and applied to experimental plots prior to each measurement campaign. These treatments were designed to simulate future atmospheric wet N deposition scenarios. The target nitrogen concentrations were calculated by applying the annual increase of 3.25% reported by Ossohou et al., 2021 to the currently measured and published nitrate (NO_3^-) and ammonium (NH_4^+) concentrations in rainfall at Lamto (Ossohou et al, 2021), Korhogo (Diaby et al, 2023), and Dahra (Laouali et al, 2021), in order to estimate projected nitrogen concentrations for the year 2050. The resulting target concentrations for each treatment are presented in Table A1 (Appendix A). Therefore, N was added according to different nitrate -to-ammonium partitioning scenario corresponding to the target nitrogen concentration ($\text{N-NO}_3^- + \text{N-NH}_4^+ = \text{N target}$). Three treatments and control were applied:

1. **Control (C):** no additional N (ambient control). Plots watered with forage water;
2. **Solution S₁ (Treatment S₁):** forage water with addition of nitrogen solution composed of 30% N- NO_3^- and 70% N- NH_4^+ ; referred to as a business-as-usual scenario, as this nitrate-to- ammonium partition reflects the current N partition in rainfall.
3. **Solution S₂ (Treatment S₂):** forage water with addition of nitrogen solution composed of 25% N- NO_3^- and 75% N- NH_4^+ ; realistic future scenario (moderate increase in ammonium dominance)
4. **Solution S₃ (Treatment S₃):** forage water with addition of solution composed of 12% N- NO_3^- and 88% N- NH_4^+ , drastic change scenario (strong dominance of reduced forms in deposition)

The watering schedule for the three study sites is summarized in Table A2 (Appendix A).

Watering volumes were calculated to be as close as possible to 3% of the annual rainfall at each site to ensure that the additional water input remained negligible relative to natural precipitation. Watering events were distributed throughout the rainy season and designed to follow the seasonal variability of the rainfall patterns at each site. The frequency and the number of



watering events were determined according the duration and distribution of the rainy seasons, as well as the number of months receiving significant precipitation.

295 2.3 Treatment protocol

Rainwater samples and local forage water were collected at each site and analyzed at the Laboratoire d'Aerologie (LAERO, Toulouse) using ionic chromatography to determine the nitrate and ammonium concentrations. All chemical analyses were performed using qualified and standardized procedures in accordance with the protocols described by Ossouhou et al. (2021) and Laouali et al. (2021).

The S_1 , S_2 and S_3 watering solutions were prepared by dissolving nitrate and ammonium salt (NH_4Cl and $NaNO_3$) in local forage water. Because forage water already contained background nitrate concentrations, site specific corrections were applied when calculating the amount of nitrates to be added.

305 At Lamto, nitrate concentrations in forage waters were low enough to avoid blank correction. In Nambekaha, forage water contained $0.171 \text{ mg L}^{-1} \text{ NO}_3^-$, consequently $0.2 \text{ mg L}^{-1} \text{ NO}_3^-$ was subtracted from the calculated nitrate addition. In Dahra, nitrate concentration in forage water reached $0.839 \text{ mg L}^{-1} \text{ NO}_3^-$ in 2024 and $0.4 \text{ mg L}^{-1} \text{ NO}_3^-$ in 2025. As for Nambekaha, these background concentrations were subtracted from the calculated nitrates to be added.

310 The nitrogenous salts were weighted and sent to the experimental sites in individual pill boxes. Each pill box contained the exact quantity of salts required to prepare 1L (by dissolution in forage water) of concentrated mother solution corresponding to S_1 , S_2 and S_3 . To obtain the final treatment concentrations, 10 mL (or 15 mL) of each mother solutions were diluted in watering cans containing 10 L of forage water (or 15 L) for Dahra and for Lamto/Nambekaha, respectively.

315 In 2025, the forage previously used in Nambekaha during 2023 and 2024 became unavailable, and water had to be collected at an alternative forage where nitrate concentration was elevated ($6.39 \text{ mg L}^{-1} \text{ NO}_3^-$). Under these conditions, it was not possible to sufficiently reduce nitrate concentrations to prepare realistic S_1 and S_2 solutions. Consequently, only S_3 treatment was prepared, without nitrate addition and using ammonium supplementation only. Therefore, during the 2025 campaign in Nambekaha, plots assigned to C, S_1 and S_2 did not received experimental watering and were exposed solely to natural rainfall.

2.4. Flux Measurement and calculation

325 Rectangular stainless-steel chambers (base 40x20cm, height 18 cm including frame) were used for flux measurements. Each chamber was mounted on a frame made of the same material, which was previously inserted about 5 cm into the soil to ensure stable installation. The frame was equipped with a water-filled groove allowing an airtight fit of the chamber and ensuring system tightness by preventing any intrusion of outside air during measurements. This chamber design is described in Serca et al., 1994. The chambers were connected to gaseous ambient air analysers by approximately 11 m of Teflon tubing. Each measurement series consisted in 10 minutes closure time to allow the accumulation of air within the chamber, followed by a purging



time of 5 minutes (Duthoit et al., 2020). This cycle of 10 minutes of accumulation and 5 minutes of ventilation was repeated for all plots, ensuring the representativeness and reproducibility of the recorded fluxes. The Picarro G2508 is a high-precision multigas analyzer that enables the simultaneous measurement of several greenhouse gases and reactive compounds, including CO₂, CH₄, NH₃, N₂O, as well as water vapor (H₂O). It was deployed across all experimental sites to specifically quantify CO₂, CH₄, and N₂O fluxes exchanged between the soil and the atmosphere.

The minimum detectable fluxes MDF were estimated at 0.0007 μg C m⁻² s⁻¹ for CO₂, 0.002 ng C m⁻² s⁻¹ for CH₄ and 0.026 ng N m⁻² s⁻¹ for N₂O. This MDF were calculated using the approach and formula described by Ba et al., 2026 based on the original method proposed by Zaman et al., 2021.

The Teledyne T200 UP is a high-precision analyser dedicated to the measurement of nitrogen oxides, particularly nitric oxide (NO), based on chemiluminescence technology (Teledyne API, 2024). The analyser has a typical detection limit of approximately 0.5 ppb for NO which correspond to a minimum detectable flux (MDF) of 0.00446 ng N m⁻² s⁻¹. It should be noted that only fluxes exceeding the detection limit of the measuring instruments are presented in the results.

Fluxes F were calculated from the linear regression of the cumulative gas concentration inside the chamber as a function of time. The slope of this linear regression, corresponding to the initial portion of the increase in the chamber (first 5-8 minutes) is (ΔC/Δt) is used in the following Eq. (1) for the flux calculation:

$$F = \frac{\Delta C}{\Delta t} \times \frac{V}{A} \times \frac{P}{R \times T} \quad (1)$$

where:

- F = gas flux (μgC m⁻² s⁻¹, ngC m⁻² s⁻¹, μgN m⁻² s⁻¹ or ng N m⁻² s⁻¹),
- ΔC/Δt = rate of change in gas concentration (ppm s⁻¹ or ppb s⁻¹),
- V = chamber volume (0.016 m³),
- A = soil surface area covered (0.08 m²),
- P = atmospheric pressure (101325 Pa),
- T = ambient temperature (306 K),
- R = universal gas constant (8.314 J mol⁻¹ K⁻¹).

Fluxes were considered valid and kept in the data set for subsequent analysis when the coefficient of determination (R²) of the linear regression exceeded 0.90 for CO₂ and NO, and 0.50 for CH₄ and N₂O. Applying the coefficient of determination (R²) criterion lead to the following statistics: in 2024, 100% of the CO₂ fluxes were validated (144 fluxes), 99% of the CH₄ fluxes (142 fluxes), 53% of the N₂O fluxes (77 fluxes) and 99% of the NO fluxes (95 fluxes : no measurements were conducted at Dahra). In 2025, 100% of the CO₂ and CH₄ measurement



were validated (144 fluxes), 80% of the N₂O fluxes (115 fluxes) and 99% of the NO fluxes (143 fluxes). Flux values were converted into mass-based units and expressed as μg C m⁻² s⁻¹ for CO₂, ng C m⁻² s⁻¹ for CH₄, and ng N m⁻² s⁻¹ for N₂O and NO.

2.5. Field Campaign Periods

Intensive measurement campaigns were conducted in 2024 and 2025 following the schedule given in Table 1.

Table 1: Schedule of intensive measurement campaigns conducted in 2024 and 2025 at the three study sites during the wet season.

Sites	2024 Campaigns	2025 Campaigns
Lamto	June 16 to 18, 2024	June 27 to 30, 2025
Nambekaha	June 22 to 25, 2024	July 3 to 7, 2025
Dahra	September 28 to October 2, 2024	September 23 to 25, 2025

(No NO/NO₂ measurements were conducted due to a malfunction of the Teledyne T200P-UP analyser.)

Flux measurements were done once in each experimental plot each year, i.e. 16 plots x 3 ecosystems x 3 sites x 2 years = 288 fluxes.

2.6. Soil moisture measurements

Soil moisture was measured simultaneously at a depth of 8 cm in the experimental plots using TMS-4 probes. These sensors, known for their accuracy and stability, record soil hydrological and thermal parameters at a 15-minute sampling frequency. The measurement depth corresponds to the most active zone of the soil in terms of respiration and microbial processes involved in the production and/or consumption of the studied gases (CO₂, CH₄, N₂O) and reactive nitrogen (NO).

Soil moisture was calculated using the following calibration Eq. (2):

$$y = ax^2 + bx + c \quad (2)$$

Where y is the soil moisture and x the registered electromagnetic pulse (Wild et al., 2019). Coefficients a , b , and c were determined according to soil composition (<https://tomst.com/web/en/systems/tms/software/>). The values corresponding to each site are reported in Table 2 and derived from the following information: At Lamto site, the soil is sandy, composed of 77% of sand, 14% of silts and 9% of clays (Abbadie et al., 2006; Srikanthasamy et al., 2018). At Nambekaha site, as the exact characteristics of the soil were not provided, we estimated that the soil is composed of 62% of sand, 14% of silts and 24% of clay (based on visual comparison with Lamto soils). Finally, at the Dahra site, the soil is composed of 89% of sand, 4.7% of silts and 6.3% of clay (Delon et al., 2022).

Table 2: Soil moisture parameters

Sites	a	b	c
-------	---	---	---



Lamto	$-1.96 \cdot 10^{-8}$	$2.68 \cdot 10^{-4}$	-0.17
Nambekaha	$-2.53 \cdot 10^{-8}$	$3.2 \cdot 10^{-4}$	-0.22
Dahra	$1.99 \cdot 10^{-8}$	$2.61 \cdot 10^{-4}$	0.16

2.6. Soil pH measurement

Soil pH measurements were conducted at the Lamto and Nambekaha sites in 2024 across the three types of vegetation (trees, grass, and crops). In each experimental plot, soil samples were collected at a depth of approximately 20 cm after removing the surface layer. Soil pH was determined using a portable soil pH meter (HI98168, Hanna Instruments) equipped with a specific electrode (HI12923) with automatic temperature compensation. Prior to measurements, the instrument was calibrated using standard buffer solutions (pH 4.01 and 7.01), and the electrode was rinsed with distilled water. In addition, a solution-based method was applied to improve accuracy: soil samples were dried and sieved to 2 mm, after which 10 g of soil were weighed and mixed with 25 mL of HI7051 extraction solution. The mixture was stirred for 30 seconds, allowed to rest for 5 minutes, and then the pH of the solution was measured. Two measurements were performed in each plot to account for spatial heterogeneity. The obtained values were then averaged at the plot scale, and an overall mean was calculated for each site by integrating the three ecosystems, in order to obtain a representative estimate of soil pH at the scale of the site.

2.7. Statistical analysis

Statistical analyses were performed using R software (version 4.5.0). The effects of soil moisture, treatments, site, and vegetation type on flux responses were evaluated using a linear model (analysis of covariance, ANCOVA).

In this framework, soil moisture was considered a continuous covariate, while control (C) and treatments (S_1 , S_2 , S_3), site (Lamto, Dahra, Nambekaha) and vegetation types (trees, grass, crops) were considered as fixed factors. It should also be noted that soil moisture data for 2024 at the Dahra site for crops were not included due to a malfunction of the TMS4 probe. The model was fitted using the ordinary least squares method, and the significance of the explanatory variables was assessed using Fisher's tests (F-tests) derived from the model ANOVA. Only main effects were considered in this model.

Collinearity among explanatory variables was assessed using the Variance Inflation Factor (VIF). A VIF value close to 1 indicates the absence of collinearity between explanatory variables, confirming that soil moisture, site, control and treatments, and vegetation type independently contribute to explaining gas fluxes. Verifying these conditions ensures the validity of the statistical tests and prevents misinterpretation ($VIF > 5$) regarding the significance of the studied factors on the measured fluxes.

When factor effects were significant, post hoc comparisons between levels were performed using estimated marginal means. The threshold for statistical significance was set at $p = 0.05$.



3. Results

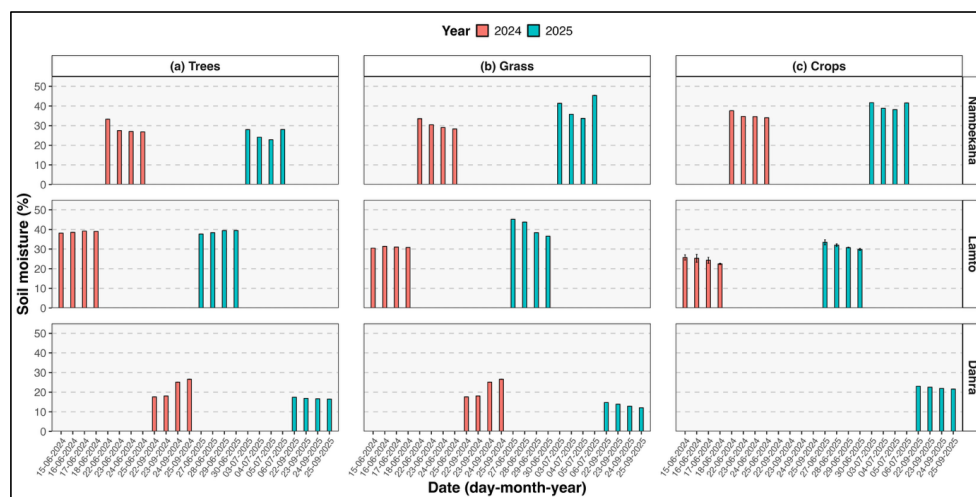
3.1. Soil moisture

The daily soil moisture levels measured during the intensive field campaigns conducted in 2024 and 2025 across the three study sites are displayed in Fig. 2. At Nambekaha site, a maximum value was recorded, reaching $45.38 \pm 0.08\%$ in 2025 (see Table B1 in Appendix B) under grass cover.

At Lamto, soil moisture in the cultivated plots in 2024 and 2025 is slightly lower compared to Nambekaha, with a maximum of $33.47 \pm 1.29\%$ in 2025 (see Table B1 in Appendix B).

In contrast, the Dahra site is characterized by much drier conditions. In the savanna, maximum soil moisture reaches only $26.58 \pm 0.05\%$, corresponding to a peak observed on 25 September 2024 (see Table B1 in Appendix B).

An interannual comparison of soil moisture was conducted for each site and ecosystem (Student's t-test, $p < 0.05$) using daily soil moisture data corresponding to the measurement campaign periods in 2024 and 2025, excluding the crop plot at Dahra due to a data issue in 2024 (Fig. 2). The results indicate significant variability in soil moisture mainly in grass and tree areas of the savanna plots (see Table B2 in Appendix B) between both years. At Lamto, soil moisture is significantly higher in 2025 than in 2024 in crop plots ($24.5 \pm 1.45\%$ in 2024 vs $31.5 \pm 1.58\%$ in 2025, $p < 0.001$) and under trees ($30.9 \pm 0.39\%$ in 2024 vs $41.0 \pm 4.17\%$ in 2025, $p = 0.017$). A significant higher soil moisture was also observed under trees at Nambekaha ($30.4 \pm 2.34\%$ in 2024 vs $39.0 \pm 5.31\%$ in 2025, $p = 0.039$), whereas at Dahra a significant lower soil moisture was recorded in the tree area ($21.8 \pm 4.67\%$ in 2024 vs $13.4 \pm 1.17\%$ in 2025, $p = 0.033$). In contrast, the grass ecosystem showed no significant interannual variation across the three sites (see Table B2 in Appendix B).



455 Figure 2: Daily soil moisture (%) at Nambekaha, Lamto and Dahra across each ecosystem: (a) Trees, (b) Grass, and (c) Crops during the field campaigns.



3.2. CO₂ fluxes

Overall, CO₂ fluxes are higher across the different ecosystems in 2025 compared to 2024 (+2 to 130%). In general, CO₂ emissions at the Dahra site across the three ecosystems, as well as in the crop system at Nambekaha, were consistently higher in 2025 than in 2024 (Fig. 3). The increase in emissions in 2025 was particularly pronounced for the S₃ treatment under trees at Lamto, which exhibited very strong interannual variability, with mean fluxes rising from $39.37 \pm 4.2 \mu\text{g C m}^{-2} \text{ s}^{-1}$ in 2024 to $91.35 \pm 73.2 \mu\text{g C m}^{-2} \text{ s}^{-1}$ in 2025 (see Table C1 in Appendix C). In addition, the analysis of spatial variability in 2024 indicates that CO₂ emissions at Dahra were the lowest compared with those measured at Nambekaha and Lamto (Fig. 3).

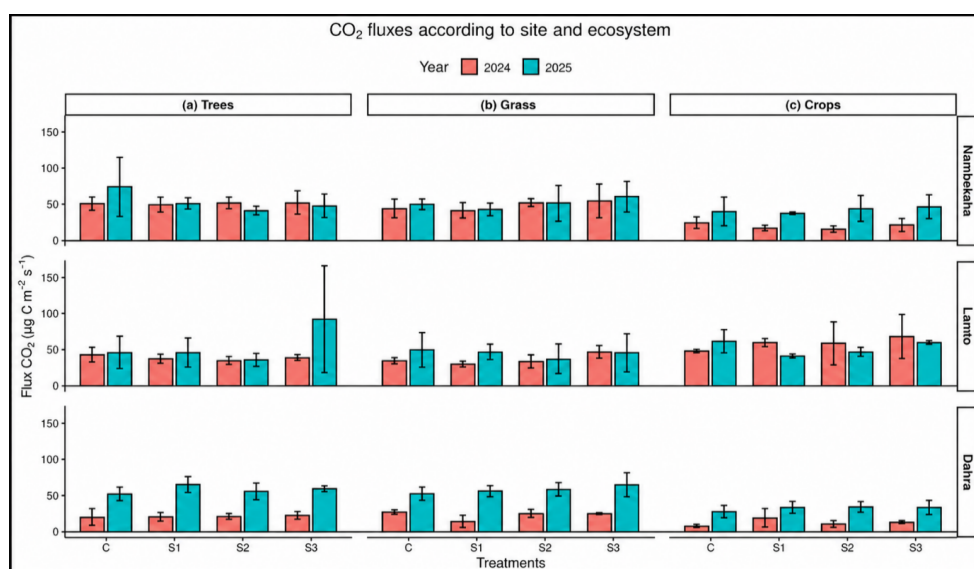
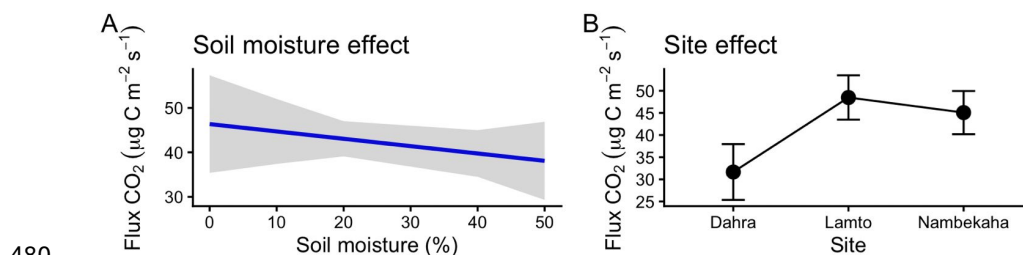


Figure 3: Interannual and spatial variation of CO₂ ($\mu\text{g C m}^{-2} \text{ s}^{-1}$) fluxes at Nambekaha, Lamto and Dahra across each ecosystem: (a) Trees, (b) Grass, and (c) Crops.

The results from the ANCOVA analysis (models) are overall significant ($p < 0.001$), although their explanatory power remains limited, with a coefficient of determination (R^2) of 0.14, indicating that only 14% of the variability in CO₂ fluxes is explained (Table 3). Collinearity analyses indicated VIF values close to 1, confirming the absence of redundancy among explanatory variables. Interactions between explanatory variables were not included because of non-significant results ($p > 0.05$, this statement is also valid for the other fluxes).

This statistical study (Table 3) showed that CO₂ fluxes decrease when soil moisture increases ($\beta = -1.105 \pm 0.236$; $p < 0.001$) (Fig.4A). The significant correlation of the site with CO₂ fluxes (Table 3) indicated that CO₂ emissions are lower in Dahra compared to Lamto ($\beta = +26.765 \pm 4.719$; $p < 0.001$) and Nambekaha ($\beta = +22.640 \pm 4.586$; $p < 0.001$) (Fig.4B). However, there was no significant effect of vegetation type or treatments on CO₂ fluxes.



480

Figure 4: Estimation of the effects of soil moisture (A) and site (B) on CO₂ fluxes

Table 3: Linear model results showing the effects of soil moisture, control and treatments, vegetation type and site location on CO₂ fluxes. The model used automatically S₁ as the reference level for treatments, crops for vegetation type, and Dahra for site. For each variable, the table reports the estimated coefficient (β : Estimate) and the p-value indicating statistical significance. Significance levels are noted: ns (not significant), * ($p < 0.05$), ** ($p < 0.01$), *** ($p < 0.001$). The R² values indicate the proportion of variance explained by the model

485

Variable	(β) Estimate (µg C m ⁻² s ⁻¹)	p-value
Treatment S ₂	+0.577 ±3.550	0.870 ns
Treatment S ₃	+8.561 ±3.550	0.016 (*)
Control C	+3.075 ±3.550	0.387 ns
Vegetation_Grass	+4.110 ±3.155	0.193 ns
Vegetation_Trees	+5.851 ±3.160	0.065 ns
Site_Lamto	+26.765 ± 4.719	3.721×10 ⁻⁸ (***)
Site_Nambekaha	+22.640 ± 4.586	1.417×10 ⁻⁶ (***)
Soil_moisture	-1.105 ± 0.236	4.536×10 ⁻⁶ (***)
R ² of the complete model	0.14	3.089×10 ⁻⁶ (***)

3.3. CH₄ fluxes

At Nambekaha, methane fluxes indicate that soils can occasionally behave as methane sources, particularly in the grass areas where emissions were higher than those observed at the other sites. The highest methane emissions were recorded in 2025 under the S₂ treatment, reaching 11.78 ± 12.2 ng C m⁻² s⁻¹, compared with 3.26 ± 2.9 ng C m⁻² s⁻¹ in 2024 (Fig. 5, Table C2). Although overall methane fluxes remained relatively low, the grass plots at Nambekaha consistently showed higher emissions than those measured at Lamto and Dahra. In contrast, crop plots at Nambekaha generally acted as weak methane sinks, though with lower uptake rates than those observed at Lamto.

490

495

At Lamto, soils generally behaved as stronger methane sinks, especially in crop plots where negative fluxes were more pronounced than at Nambekaha. The strongest methane uptake was measured in 2025 in the crop plot under the S₃ treatment, with a flux of -4.94 ± 1.9 ng C m⁻² s⁻¹ (Fig. 5, Table C2). These results suggest a greater methane consumption capacity in Lamto soils, particularly under cultivated conditions. Methane emissions from grass areas in Lamto remained lower than those observed at Nambekaha.

500

Finally, at Dahra, methane fluxes remained very low and were generally close to zero (Fig. 5). This indicates that soils at this site behaved as nearly neutral systems with respect to methane



505 exchange, showing neither strong emissions nor substantial methane uptake compared with the other two sites.

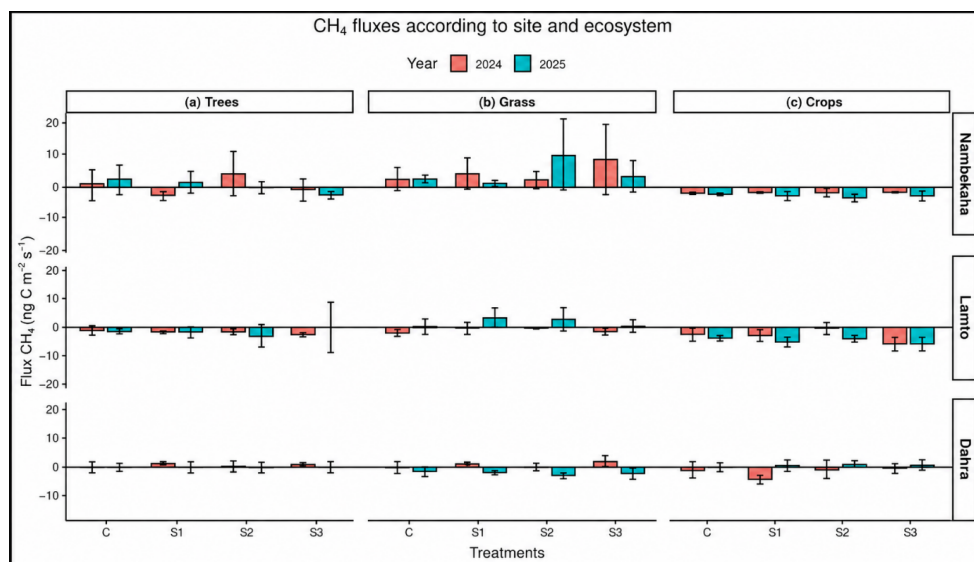


Figure 5: Interannual and spatial variation of CH₄ (ng C m⁻² s⁻¹) fluxes at Nambekaha, Lamto and Dahra across each ecosystem: (a) Trees, (b) Grass, and (c) Crops.

510 A similar statistical analysis without the 2024 soil moisture data in the Dahra crop and without
 interaction between explanatory variables ($p > 0.05$), based on linear models applied to CH₄
 fluxes showed that the models are globally significant ($p < 0.001$), with a R^2 of 0.21 indicating
 that 21% of the variability in CH₄ fluxes is explained (Table 4). Collinearity analyses also
 indicated VIF values close to 1, confirming the absence of redundancy among explanatory
 515 variables.

This study showed a strong effect of the vegetation type on CH₄ fluxes. (Fig.6A, Table 4), with
 higher emissions under trees than in crops ($\beta = +1.932 \pm 0.62$; $p < 0.001$) and even larger
 emissions (Fig.6A) in grass area ($\beta = +3.836 \pm 0.62$; $p < 0.001$, Table 5). The statistical analysis
 also showed a significant effect of the site on CH₄ fluxes ($\beta = -2.1454 \pm 0.92$; $p < 0.05$) indicating
 520 uptake in Lamto, emissions in Nambekaha and low fluxes close to zero at Dahra (Fig.6B). No
 significant effect of soil moisture and treatments on CH₄ fluxes was observed.

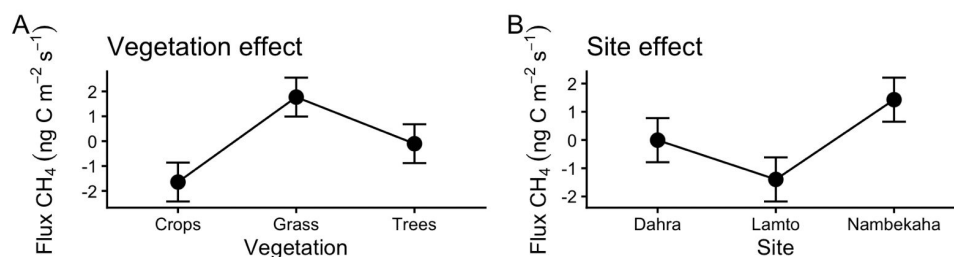


Figure 6: Estimation of the effects of vegetation type (A) and site (B) on CH₄ fluxes

525 Table 4: Linear model showing the effects of soil moisture, control and treatments, vegetation type and site location on CH₄ fluxes. The model used automatically S₁ as the reference level for treatments, crops for vegetation type, and Dahra for site. For each variable, the table reports the estimated coefficient (Estimate) and the p-value indicating statistical significance. Significance levels are noted: ns (not significant), * (p < 0.05), ** (p < 0.01), *** (p < 0.001). The R² values indicate the proportion of variance explained by each model.

Variable	(β) Estimate	p-value
Treatment S ₂	+0.725±0.70	0.301 ns
Treatment S ₃	-0.028±0.68	0.967 ns
Control C	+0.067±0.70	0.923 ns
Vegetation_Grass	+3.835±0.62	2.932×10 ⁻⁹ (***)
Vegetation_Trees	+1.932±0.62	0.0019 (**)
Site_Lamto	-2.145±0.92	0.021 (*)
Site_Nambekaha	+0.744±0.89	0.406 ns
Soil_moisture	+0.073±0.04	0.113 ns
R ² of the complete model	0.21	3.629×10 ⁻¹⁰ (***)

530 3.4. N₂O fluxes

The statistical model applied to N₂O fluxes does not show any significant impact of soil moisture, control and treatments, vegetation or site (p > 0.05), therefore the table of statistical results is not shown. Despite that, across all studied sites, N₂O fluxes exhibit strong spatial and interannual variability, with contrasting behaviors depending on control and treatments, vegetation type and sites.

535

At Nambekaha, the tree area is characterized by predominantly negative N₂O fluxes in both study years, reflecting an overall sink behavior. In contrast, cultivated plots exhibit the highest N₂O emissions compared to the three different sites, particularly in 2024, with elevated fluxes under the C plot (27.12 ± 8.5 ng N m⁻² s⁻¹) and S₃ (22.66 ± 25.1 ng N m⁻² s⁻¹). A reduction in emissions is observed in 2025, notably under S₃ (see Table C3 in Appendix C).

540

At Lamto, N₂O fluxes are generally negative, particularly in 2024, indicating that soils predominantly function as N₂O sinks (Fig. 7). This pattern is especially pronounced in the grass area, where sink strength was lower in 2025 compared to 2024 (Fig. 7b). A more moderate reduction in sink strength is also observed in the tree area (Fig. 7a), particularly under S₃, with uptake amplitude declining from -14.86 ± 4.5 ng N m⁻² s⁻¹ in 2024 to -7.99 ± 1.4 ng N m⁻² s⁻¹

545



in 2025 (see Table C3 in Appendix C). Despite the dominance of negative fluxes, a few episodic N₂O emissions are detected in 2025, mainly in the tree area under the S₂ treatment.

In maize-cultivated plots, fluxes display greater variability: N₂O emissions are observed in 2024 across control and all treatments, whereas in 2025 the soil behaves as an N₂O sink regardless of the applied treatments (Fig. 7c).

At Dahra, in the tree area, positive emissions are recorded in 2024 under the control (C), S₁ and S₂ treatments, whereas the S₃ treatment stands out with negative fluxes (Fig. 7a, Table C3). In 2025, control and all treatments show fluxes close to zero or negative.

In the grass area, N₂O fluxes are predominantly negative for control and all treatments in both years (Fig. 7b). However, sink strength is markedly lower in 2025 than in 2024.

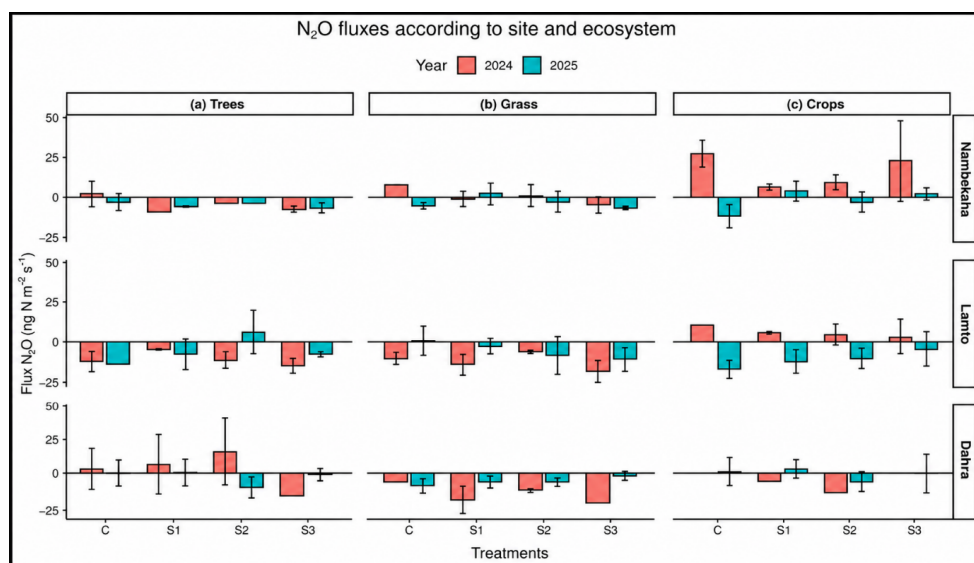


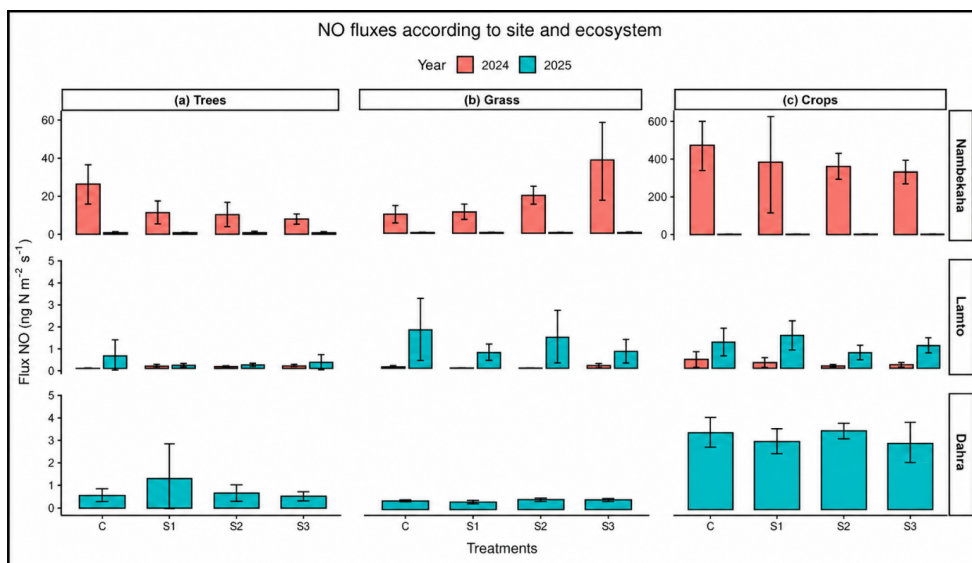
Figure 7: Interannual and spatial variation of N₂O fluxes (ng N m⁻² s⁻¹) at Nambekaha, Lamto and Dahra across each ecosystem: (a) Trees, (b) Grass, and (c) Crops.

3.5. NO fluxes

The year 2024 at Nambekaha was characterized by particularly high NO emissions compared to 2025, especially in the crop plots (Fig. 8), with fluxes ranging from 383.88 ± 74.0 ng N·m⁻²·s⁻¹ under S₃ treatment to 497.39 ± 146.3 ng N·m⁻²·s⁻¹ under the control (C) (see Table C4 in Appendix C).

In contrast, at Lamto, the highest fluxes were recorded in 2025 (Fig. 8), reaching up to 1.68 ± 1.4 ng N·m⁻²·s⁻¹ in the grass area under the control (C) (see Table C4 in Appendix C).

At Dahra 2025, higher emissions are observed in the crop plots, where they reach a maximum of 3.37 ± 0.3 ng N·m⁻²·s⁻¹ under the S₂ treatment (Fig. 8, Table C4).



570 Figure 8: Interannual and spatial variation of NO fluxes ($\text{ng N m}^{-2} \text{s}^{-1}$) at Nambekaha, Lamto and Dahra across each ecosystem: (a) Trees, (b) Grass, and (c) Crops.

The same statistical analysis without 2024 data in Dahra (due to a failure of the analyser) and without interaction between explanatory variables ($p > 0.05$), based on linear models applied to NO fluxes, showed that the models are globally significant ($p < 0.001$), with a R^2 of 0.22, indicating that 22% of the variability in NO fluxes is explained (Table 5). Collinearity analyses indicated VIF values close to 1, confirming the absence of redundancy among explanatory variables.

575 The statistical study showed a strong and significant correlation between NO fluxes and vegetation type, indicating extremely high emissions in crops compared to trees or grass ($\beta = +76.779 \pm 15.82$; $p < 0.001$) (Fig.9A, Table 5). This statistical study also showed a significant effect of the site on NO fluxes, indicating higher emissions at Nambekaha ($\beta = +72.153 \pm 14.45$; $p < 0.001$) (Fig.9B). No significant effect of soil moisture, control and all treatments on NO fluxes was observed (Table 6).

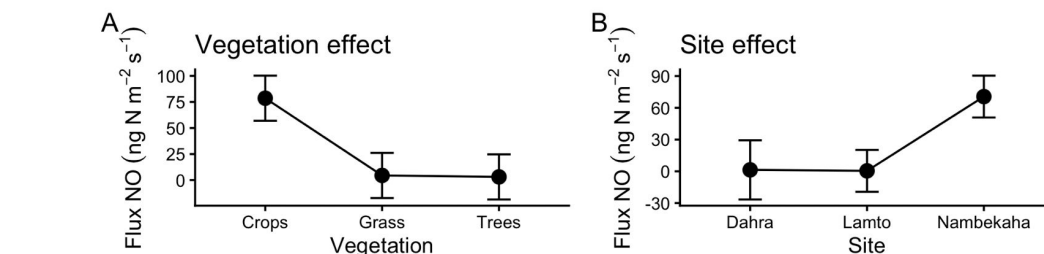


Figure 9: Estimation of the effects of vegetation type (A) and site (B) on NO fluxes

585 Table 5: Linear model results showing the effects of soil moisture, control and treatments, vegetation type and site on NO fluxes. The model used automatically S_1 as the reference level for treatments, grass



590 for vegetation type, and Lamto for site. For each variable, the table reports the estimated coefficient (Estimate) and the p-value indicating statistical significance. Significance levels are noted: ns (not significant), * ($p < 0.05$), ** ($p < 0.01$), *** ($p < 0.001$). The R^2 values indicate the proportion of variance explained by each model.

Variable	(β) Estimate	p-value
Treatment S ₂	-1.323±18.25	0.942 ns
Treatment S ₃	-6.883±18.34	0.707 ns
Control C	+7.549±18.33	0.680 ns
Vegetation_Crops	+76.779±15.82	2.286×10 ⁻⁶ (***)
Vegetation_Trees	-0.019±15.79	0.999 ns
Site_Dahra	+23.800±25.93	0.359 ns
Site_Nambekaha	+72.153±14.456	1.195×10 ⁻⁶ (***)
Soil_moisture	+1.353±1.160	0.244 ns
R ² of the complete model	0.22	2.679×10 ⁻⁹ (***)

4. Discussion

4.1. Soil CO₂ emission

600 Soil moisture exerted a significant control on CO₂ fluxes ($\beta = -1.105 \pm 0.236$; $p < 0.0001$), indicating that an increase in soil moisture (1%) is associated with an average decrease of
 595 $-1.105 \pm 0.236 \mu\text{g C m}^{-2} \text{ s}^{-1}$ in CO₂ emissions. This negative relationship suggests that increasing soil moisture limits oxygen diffusion within soil pores and decreases gas diffusivity. These physical effects therefore lead to a reduction in aerobic microbial activity and respiration (Linn and Doran, 1984; Moyano et al., 2013; Reichstein et al., 2003). This statement is especially true for soils that have already been moistened, which is the case for our
 600 measurements collected during the wet season. Such responses are particularly observed in tropical soils, where soil moisture conditions play a key role in controlling carbon mineralization (Davidson and Verchot, 2000). Furthermore, site effect is also significant: CO₂ emissions were lower at Dahra compared to Lamto and Nambekaha, likely due to lower organic carbon availability. A contextual factor may also explain part of the higher CO₂ fluxes observed
 605 in 2024 compared to 2025 at Lamto. Indeed, the maize field had been tilled prior to the measurement campaign, which likely improved soil aeration and promoted aerobic conditions favorable to microbial activity and organic matter decomposition. This process can temporarily stimulate soil respiration and increase CO₂ emissions. Such effects are well documented, with several studies showing that tillage significantly increases CO₂ fluxes by enhancing microbial
 610 access to organic carbon and altering soil structure (Abdalla et al., 2016; Liu et al., 2022).

4.2. Soil CH₄ emission and uptake

615 For CH₄, vegetation type appeared to be the primary determinant of fluxes. Grass areas exhibited CH₄ emissions ($+3.836 \pm 0.62 \text{ ng C m}^{-2} \text{ s}^{-1}$), whereas crops tended to act as methane sinks. These differences likely reflect variations in soil structure, porosity, and methanotrophic activity across vegetation types (Le Mer and Roger, 2001; Liu et al., 2022). Tree areas showed a more moderate effect ($+1.932 \pm 0.62 \text{ ng C m}^{-2} \text{ s}^{-1}$ relative to crops). These patterns likely reflect differences in soil aeration and redox potential, that regulate the balance between



methanogenesis and methanotrophy (Le Mer and Roger, 2001). The comparison of the site effect on CO₂ and CH₄ fluxes highlights the existence of an opposite behaviour between these two gases. Indeed, the Lamto site, characterized by high CO₂ emissions, shows a strong CH₄ uptake. According to Liu et al. (2022), CH₄ oxidation by methanotrophs is closely linked to total soil respiration, estimated from CO₂ emissions. Their study indeed reported a negative correlation: when heterotrophic respiration increases, the soil capacity to consume atmospheric methane increases (i.e. the methane uptake increases), likely due to competition for substrates or micronutrients. This relationship indicates that carbon-driven microbial activity can modulate the role of soils as CH₄ sinks.

4.3. Soil N₂O emission and uptake

Regarding N₂O, ANCOVA and linear models indicate that neither treatment, nor soil moisture, nor vegetation type significantly explained the variability in N₂O fluxes ($p > 0.05$), suggesting that factors typically associated with N₂O production and uptake did not exert a clear influence on N₂O fluxes during the study periods. Indeed, many studies indicate that N₂O emissions are often dominated by "hot spots" and "hot periods," making it difficult to identify clear statistical relationships with average environmental variables (Groffman et al., 2009). The absence of significant statistical results in our study is consistent with this. It should be noted that N₂O emissions observed in 2024 in the Nambekaha field are linked to the fertilization with 150 kg NPK ha⁻¹ independently of experimental treatments. Several studies have shown that nitrogen fertilization in agricultural soils significantly enhances N₂O emissions by increasing nitrogen substrate availability for nitrification and denitrification processes (Bouwman et al., 2002; C. Wang et al., 2021)

Two main linked processes may explain negative N₂O fluxes in soils with low N content: 1- N₂O from the soil gaseous phase is reduced to N₂ by denitrification, *i.e.* N₂O is consumed, and 2- Atmospheric N₂O is transported within the soil profile via passive diffusion and convection depending on oxygen conditions (which also drives nitrification and denitrification processes, Clough et al., 2005).

Even under predominantly aerobic conditions, soils can exhibit negative N₂O fluxes, reflecting net consumption of the gas by the soil. Indeed, several studies have shown that N₂O consumption (driven by denitrification) is not exclusively limited to saturated soils but can also occur in generally well-aerated soils (Dlamini et al., 2024). For example, Bateman and Baggs, (2005) demonstrated that soils considered as aerobic can exhibit net N₂O consumption due to micro-anoxic zones associated with moisture and structural aggregation. Within these microenvironments, oxygen diffusion is locally restricted, while microbial respiration rapidly consumes available O₂, creating conditions favorable for complete denitrification and enhanced reduction of N₂O to N₂. These conditions may contribute to very low N₂O emissions or even occasional net N₂O consumption. Similarly, Groffman et al. (2009) observed comparable processes in well-drained agricultural soils, where soil structure and microbial activity generated anaerobic microsites capable of supporting N₂O complete reduction despite an overall oxic environment. Ideal conditions for N₂O emissions are not found in these particular



cases. However, Chapuis-Lardy et al (2007, and references therein) mention that it is difficult to clearly define a set of conditions promoting N₂O consumption.

660 In our results, the fact that mean volumetric soil moisture did not emerge as a significant factor does not necessarily imply the absence of conditions favorable to denitrification but may reflect the microscopic and spatially heterogeneous nature of anaerobic zones (replicates in experimental protocol may however reduce this heterogeneity). Soil redox status must therefore be considered at the fine scale of aggregates and pores, where small local variations in oxygen
665 can reverse the net N₂O balance.

Furthermore, N₂O diffusion in the soil seem to enhance N₂O consumption (Chapuis-Lardy et al., 2007, and references therein) associated with low N availability in soils and aerobic denitrification in well aerated soils. In our case, episodes of N₂O consumption could be explained by similar conditions, notably mineral nitrogen limitation and low soil moisture (in
670 comparison to temperate or boreal soils). Savage et al. (2014) demonstrated the existence of significant net N₂O consumption in a semi-arid agricultural site of North Dakota, highlighting that high-frequency measurements are essential to detect low or transient fluxes, which may explain their scarcity in the tropical literature. In addition, Dijkstra et al. (2013) and Wu et al. (2013) highlighted the capacity of certain terrestrial ecosystems, particularly nitrogen-poor soils
675 under relatively dry conditions, to consume atmospheric N₂O (reduction of N₂O to N₂ can exceed its local production when mineral nitrogen availability is limited), challenging the assumption of a strict dependence on anaerobic microsites.

4.4. Soil NO emission

The absence of a significant relationship between NO emissions and soil moisture suggests that
680 soil moisture is not the primary driver of NO production in this study, although its influence cannot be considered negligible. Instead, NO emissions appear to be more strongly controlled by nitrogen substrate availability and microbial processes involved in the nitrogen cycle. Considering the vegetation effect, crop plots showed significantly higher NO emissions than tree areas ($\beta = +76.799 \pm 15.96$; $p < 0.0001$), while no significant difference was observed
685 between grass and tree areas. This reflects the influence of agricultural practices, particularly of fertilizer inputs. Indeed, in the crop plot at Nambekaha, a fertilization of approximately 150 kg NPK ha⁻¹ was applied independently of experimental treatments in 2024. This resulted in greater mineral nitrogen availability, thereby enhancing nitrification (Skiba et al., 1997; Butterbach-Bahl et al., 2013) and NO emissions. Recent studies have shown that increased
690 nitrogen fertilizer inputs in agricultural systems lead to significant increases in soil nitrogen emissions, particularly NO, due to excess substrate availability for nitrification (Bratti et al., 2022; Gong et al., 2025). In 2025, no fertilization was applied by the farmers at Nambekaha prior to our field campaigns.

The effect of site location on NO emissions shows higher emissions at Nambekaha than at
695 Lamto and Dahra, (due to 150 kg NPK ha⁻¹ fertilisation in 2024 at the Nambekaha cropland site). Furthermore, the low NO emissions at Lamto (site effect) in grass area (vegetation effect)



corroborate the inhibition of nitrification by dominant grasses in Lamto (Srikanthasamy et al., 2018) subsequently limiting NO_3^- availability and NO emissions.

700 A methodological limitation should nevertheless be acknowledged: during chamber
measurements, nitric oxide may react with ozone within the chamber headspace,
potentially leading to an underestimation of NO fluxes if ozone concentrations are sufficiently
high (Ludwig et al., 2001; Pape et al., 2009; Williams and Davidson, 1993). Because ozone
concentrations were not measured during the field campaigns, no correction were applied.
705 Previous studies have shown that this effect can lead to an average underestimation of NO
fluxes of approximately 30%, although the magnitude of the bias depends on seasonal
conditions (Delon et al., 2017). However, the relatively short chamber closure time reduced the
residence
time of air inside the chamber, the chamber walls are opaque, thereby limiting the extent of this
reaction. Moreover, the same measurement protocol was applied consistently across all
710 treatments and sites, suggesting that any potential bias was systematic rather than treatment-
specific and therefore unlikely to alter the relative differences among treatments or the
conclusions of the statistical analyses.

4.5. Treatment effect

715 Control (C) and treatments (S_1 , S_2 , S_3) showed no significant effect on CO_2 , CH_4 , N_2O or NO
fluxes, regardless of the treatment applied. This lack of effect may indicate that nitrogen inputs
were insufficient to significantly alter microbial activity and increase emissions. It may also
reflect a dominant control by environmental factors, such as soil moisture, site location and
vegetation type, which can mask treatments effects, as observed in some low-input tropical
ecosystems (Butterbach-Bahl et al., 2013).

720 4.6. Comparison with other studies

Due to the weak temporal extension of our field results, a generalisation of these processes
leading to N_2O negative fluxes should be taken with caution. Overall, despite the short-term
character of the field campaigns, the results provided in this study are generally in line with
other studies conducted in tropical African ecosystems (Table 6). The CO_2 fluxes measured at
725 Dahra (12.59 ± 8.0 to $57.83 \pm 10.4 \mu\text{g C m}^{-2} \text{ s}^{-1}$ depending on vegetation type) are higher than
those reported by Assouma et al., 2017 in similar Sahelian pastures ($12.29 \pm 2.3 \mu\text{g C m}^{-2} \text{ s}^{-1}$).
Compared to the humid tropical conditions reported by Daelman et al., (2025) in the Congo
Basin ($48.5 \pm 13.9 \mu\text{g C m}^{-2} \text{ s}^{-1}$), our values at Nambekaha and Lamto (36.10 ± 9.2 to 58.24 ± 22.5
 $\mu\text{g C m}^{-2} \text{ s}^{-1}$) fall within a similar range. In contrast, lower mean CO_2 fluxes have been reported
730 in Kenyan savanna soils by Leitner et al., 2024 ($6.19 \pm 5.06 \mu\text{g C m}^{-2} \text{ s}^{-1}$).

The CH_4 fluxes obtained in this study (generally ranging from slight uptake to low emissions)
are of the same order of magnitude as those reported by Wieckowski et al. (2026) and Assouma
et al. (2017) at Dahra, which also describe low fluxes alternating between modest emissions
and net uptake. Our results are also consistent with the near-neutral balances observed by
735 Leitner et al. (2024) in savanna soils in Kenya ($0.028 \pm 0.194 \text{ ng C m}^{-2} \text{ s}^{-1}$). In contrast, in the



Congo Basin, Daelman et al. (2025) reported a more pronounced CH₄ uptake (-12.4 ± 16.5 ng C m⁻² s⁻¹).

740 Conversely, N₂O emissions observed by Wieckowski et al. (2026) (33.0 ± 29.8 in open grazed to 40.66 ± 34.7 ng N m⁻² s⁻¹ near the trees) and Assouma et al. (2017) (6.63 ± 0.7 in tree
plantation to 17.68 ± 5.9 ng N m⁻² s⁻¹ in pastures) at Dahra are generally higher than those measured in our study, where fluxes above the minimal detectable flux observed elsewhere were frequently negative or close to zero. Similarly, Daeman et al. (2025) reported positive N₂O emissions in the Congo Basin (11.4 ± 13.0 ng N m⁻² s⁻¹ in the Congo basin), and Leitner et al. (2024) observed low but positive mean fluxes (0.69 ± 0.61 ng N m⁻² s⁻¹ in savanna soils). Their
745 study at Dahra also reported relatively low N₂O emissions, ranging from 3.2 ± 1.7 ng N m⁻² s⁻¹ to 5.5 ± 1.3 ng N m⁻² s⁻¹.

The NO fluxes measured in our study (up to 411.9 ± 180.3 ng N m⁻² s⁻¹ in croplands at Nambekaha) show substantial variability depending on land use. These values partly overlap with those reported by Delon et al. (2017) at Dahra (6.8 ± 3.4 to 60.3 ± 26.1 ng N m⁻² s⁻¹),
750 although our maximum values in croplands exceed this range, likely due to the effects of fertilization (150 kg NPK ha⁻¹) applied to cultivated soils at Nambekaha.

The comparison of flux magnitude in semi natural grasslands (under trees and grasses) and human managed lands (crops) calls for a spatialization to explore the respective weights of each land in the net exchange of gases at the soil-atmosphere interface, as well as an extension in
755 time (our measurements were done during the wet season). Furthermore, forest areas would also need to be included to improve and supplement this study.



Table 6: Comparative flux values between other studies

	Sites	CO ₂ (µg C m ⁻² s ⁻¹)	CH ₄ (ng C m ⁻² s ⁻¹)	N ₂ O (ng N m ⁻² s ⁻¹)	NO (ng N m ⁻² s ⁻¹)
This study	Nambekaha (Côte d'Ivoire)	50.94±11.8 to 53.47±25.6 Trees	0.66±4.0 to 0.86±5.7 Trees	-4.53±4.0 to -4.35±6.1 Trees	0.65±0.3 to 13.68±10.1 Trees
		47.98±15.4 to 51.18±18.1 grass	5.35±7.8 to 5.61±7.8 grass	-3.51±5.5 to -1.11±6.0 grass	0.37±0.2 to 20.40±16.7 grass
		19.56±7.6 to 41.83±15.9 crops	-2.49±1.1 to - 1.42±0.7 crops	-1.36±7.8 to 15.49±16.7 crops	2.42±1.01 to 411.92±180.3 crops
	Lamto (Côte d'Ivoire)	38.57±7.3 to 54.59±45.1 Trees	-1.35±4.2 to - 1.53±0.9 Trees	-10.90±5.8 to -5.08±10.8 Trees	0.06±0.1 to 0.27±0.4 Trees
		36.10±9.2 to 44.80±21.5 grass	1.49±2.9 to -0.85±1.3 grass	-13.15±6.9 to -6.50±10.6 grass	0.04±0.1 to 1.08±1.0 grass
		52.36±12.1 to 58.24±22.5 crops	-4.03±1.5 to - 2.49±2.5 crops	-11.10±9.3 to 4.90±7.3 crops	0.19±0.2 to 1.09±0.6 grass
	Dahra (Senegal)	21.12±7.5 to 57.83±10.4 Trees	0±1.4 to 0.60±1.2 Trees	-2.48±7.7 to 1.82±17.7 Trees	0.77±0.9 Trees
		22.58±7.2 to 56.93±12.0 grass	-1.59±1.2 to 0.68±1.4 grass	-13.69±6.9 to -5.60±4.0 grass	0.41±0.1 grass
		12.59±8.0 to 32.04±8.7 crops	-1.08±2.2 to 0.52±1.3 crops	-8.55±3.3 to -2.82±8.4 crops	3.14±0.6 crops
Ba et al., 2026	Niakhar (Senegal)	12.7 ± 10.4 in full sun (FS) on groundnut crops 18.5±12.7 under F. albida canopy shade (Sh) on groundnut crops			
Wieckowski et al., 2026	Dahra (Senegal)	8.54 ± 74.5 near the Trees -40.8 ± 76.0 in open grazed	3.31 ± 6.0 near the Trees -0.60 ± 2.7 in open grazed	40.66 ± 34.7 near the Trees 33.0 ± 29.8 in open grazed	
Daelman et al., 2025	Yangambi (Congo)	48.5±13.9 in the Congo Basin	-12.4±16.5 in the Congo Basin	11.4±13.0 in the Congo Basin	
Assouma et al., 2017	Dahra (Senegal)	7.10 ± 0.4 in forest plantation 12.29 ± 2.3 in pastures	0.87 ± 0.9 in forest plantation 5.21 ± 3.5 in pastures	6.63 ± 0.7 in forest plantation 17.68 ± 5.9 in pastures	
Leitner et al., 2024	Kapiti (Kenya)	6.19±5.06 savanna soils	0.028±0.194 savanna soils	0.69±0.61 savanna soils	
Delon et al., 2017	Dahra (Senegal)			3.2 ± 1.7 to 5.5 ± 1.3	6.8 ± 3.4 to 60.3 ± 26.1
Otieno et al., 2010	In Ruma National Park (Kenya)	201.6±13.2 reduced rainfall to 0% on Black cotton clay soils 150±13.2 reduced rainfall to 20% on Black cotton clay soils			



765 Conclusion

This study reveals that soil moisture and site location are the primary drivers of CO₂ fluxes, while vegetation type and site location significantly influence CH₄ and NO fluxes. Contrary to initial assumptions, vegetation type does not universally control gas exchanges across all compounds. Additionally, soil moisture only strongly regulates CO₂ fluxes, and its role in governing CH₄ or NO emissions remains insignificant in our experiments conducted during the wet season. At Dahra, the driest site, fluxes of all gases were the lowest, but this observation neither confirms nor denies the hypothesis that soil moisture is a major controller of flux magnitude. Furthermore, the partitioning between nitrates and ammonium in experimental treatments had no detectable effect on flux magnitudes, likely due to the low nitrogen inputs applied during the experiments.

Soil moisture emerges as the key controlling factor for CO₂ fluxes, primarily by limiting microbial respiration under water-saturated conditions through reduced oxygen diffusion. In contrast, the absence of a significant relationship between soil moisture and NO or CH₄ fluxes suggests that these gases are instead regulated by substrate availability and specific microbial processes. For CH₄, vegetation type played a dominant role: grass-dominated areas acted as net sources, while cropped areas generally functioned as methane sinks, likely due to differences in soil structure and methanotrophic microbial activity. Site location also had a significant effect on all three gases, with the Sahelian site (Dahra) exhibiting the lowest CO₂ and CH₄ flux intensities. In Lamto, low NO emissions were attributed to nitrification inhibition under dominant grasses. These findings could be used to propose future strategies aimed at mitigating climate change in West Africa, in the context of land-use change: a balance could be struck between 1) converting savannas into cropland, which would increase CH₄ uptake, and 2) optimizing crop management to reduce N₂O and CO₂ emissions.

N₂O fluxes presented a distinct pattern, with low or even negative values across all treatments. No significant relationships were observed between N₂O fluxes and soil moisture, vegetation type, site location, or nitrogen treatments. These results indicate that the studied soils can temporarily act as N₂O sinks under certain environmental conditions, potentially driven by localized microbial activity (where N₂O consumption exceeds production), soil structural heterogeneity, and the nitrogen-poor, relatively dry nature of these soils.

The observed patterns of greenhouse gas and reactive nitrogen fluxes underscore the complex interactions between the carbon and nitrogen cycles in these ecosystems. They emphasize the critical role of microsite conditions and nitrogen availability in regulating the intensity of gas exchange between soil and atmosphere. These findings call for further investigation into microbial populations and their functional roles in nitrogen and carbon cycling to disentangle the bacterial vs. environmental processes underlying trace gas exchanges.

Overall, the results highlight that ecosystem characteristics—strongly influenced by site location—shape greenhouse gas and nitrogen fluxes, while also suggesting that classical environmental drivers may not reliably predict N₂O dynamics in tropical West African regions. These insights contribute to a more nuanced understanding of the factors controlling gas exchanges across diverse land-use systems (and their representation in model parameterizations



where N₂O uptake is not predicted) and stress the need for microscale and microbial-focused research to improve predictive models.

810

815

820

825

830



Appendix

835 Appendix A: The watering schedule for the three sites

Table A1: Nitrates and ammonium concentrations in each watering solution to achieve the nitrogen target concentration

Site	C(mgN.L ⁻¹)	S ₁ (mgN.L ⁻¹)	S ₂ (mgN.L ⁻¹)	S ₃ (mgN.L ⁻¹)
Nambekaha (target: 0.963 mgN.L ⁻¹)	2023 and 2024: $\begin{cases} N - NO_3^- = 0.039 \\ N - NH_4^+ = 0 \end{cases}$ 2025: $\begin{cases} N - NO_3^- = 1.442 \\ N - NH_4^+ = 0.051 \end{cases}$	2023, 2024 and 2025: $\begin{cases} N - NO_3^- = 0.289 \\ N - NH_4^+ = 0.674 \end{cases}$	2023, 2024 and 2025: $\begin{cases} N - NO_3^- = 0.241 \\ N - NH_4^+ = 0.722 \end{cases}$	2023, 2024 and 2025: $\begin{cases} N - NO_3^- = 0.116 \\ N - NH_4^+ = 0.847 \end{cases}$
Lamto (target: 0.966 mgN.L ⁻¹)	2023 and 2024: $\begin{cases} N - NO_3^- = 0 \\ N - NH_4^+ = 0 \end{cases}$ 2025: $\begin{cases} N - NO_3^- = 0 \\ N - NH_4^+ = 0 \end{cases}$	2023, 2024 and 2025: $\begin{cases} N - NO_3^- = 0.290 \\ N - NH_4^+ = 0.676 \end{cases}$	2023, 2024 and 2025: $\begin{cases} N - NO_3^- = 0.242 \\ N - NH_4^+ = 0.724 \end{cases}$	2023, 2024 and 2025: $\begin{cases} N - NO_3^- = 0.116 \\ N - NH_4^+ = 0.850 \end{cases}$
Dahra (target: 1.676 mgN.L ⁻¹)	2023 and 2024: $\begin{cases} N - NO_3^- = 0.189 \\ N - NH_4^+ = 0 \end{cases}$ 2025: $\begin{cases} N - NO_3^- = 0.090 \\ N - NH_4^+ = 0.078 \end{cases}$	2023, 2024 and 2025: $\begin{cases} N - NO_3^- = 0.503 \\ N - NH_4^+ = 1.173 \end{cases}$	2023, 2024 and 2025: $\begin{cases} N - NO_3^- = 0.419 \\ N - NH_4^+ = 1.257 \end{cases}$	2024 and 2025: $\begin{cases} N - NO_3^- = 0.201 \\ N - NH_4^+ = 1.475 \end{cases}$

840

845

850



Table A2: Dates of watering and flux measurements for each site. * in 2025, only solution S₃ was used in Nambekaha.

Site	Dates of watering	Dates of flux
Lamto	16 in 2023: 02/04, 18/04, 02/05, 16/05, 30/05, 06/06, 20/06, 04/07, 18/07, 01/08, 15/08, 05/09, 19/09, 03/10, 17/10, 07/11	16 in 2023: 03/04, 04/04, 03/05, 04/05, 08/06, 09/06, 05/07, 06/07, 02/08, 03/08, 06/09, 07/09, 03/10, 04/10, 08/11, 09/11
	16 in 2024: 12/03, 26/03, 09/04, 23/04, 02/05, 16/05, 30/05, 11/06, 25/06, 09/07, 23/07, 13/08, 12/09, 03/10, 17/10, 05/11	3 in 2024: 16/06, 17/06, 18/06
	13 in 2025: 15/03, 25/03, 10/04, 22/04, 07/05, 21/05, 03/06, 23/06, 08/07, 22/07, 05/08, 02/09	4 in 2025: 27/06, 28/06, 29/06, 30/06
Nambekaha*	14 in 2023: 29/05, 05/06, 19/06, 03/07, 13/07, 24/07, 03/08, 14/08, 23/08, 04/09, 12/09, 23/09, 02/10, 16/10	
	14 in 2024: 15/04, 06/05, 20/05, 10/06, 27/06, 11/07, 22/07, 01/08, 12/08, 22/08, 02/09, 16/09, 30/09, 14/10	4 in 2024: 22/06, 23/06, 24/06, 25/06
	6 in 2025: 14/04, 28/04, 12/05, 26/05, 09/06, 23/06	4 in 2025: 03/07, 04/07, 05/07, 06/07
Dahra	7 in 2023: 14/07, 28/07, 11/08, 23/08, 08/09, 20/09, 18/10	
	7 in 2024: 16/07, 29/07, 12/08, 26/08, 10/09, 25/09, 09/10	3 in 2024: 23/09, 24/09, 25/09
	6 in 2025: 14/07, 29/07, 12/08, 26/08, 09/09, 20/09	4 in 2025: 22/09, 23/09, 24/09, 25/09

855

860



Appendix B: Soil moisture in the studied ecosystems: daily averages and interannual comparison (2024–2025)

Table B1: Average daily soil moisture for 2024 and 2025 across the 3 ecosystems of the three sites

	Average soil moisture (%) 2024				Average soil moisture (%) 2025			
Nambekaha (Trees)	22/06/2024 33.30±0.04	23/06/2024 27.48±0.00	24/06/2024 27.02±0.00	25/06/2024 26.83±0.00	03/07/2025 27.97±0.03	04/07/2025 24.13±0.01	05/07/2025 22.82±0.02	06/07/2025 28.01±0.03
Nambekaha (Grass)	22/06/2024 33.60±0.02	23/06/2024 30.45±0.00	24/06/2024 29.07±0.00	25/06/2024 28.29±0.00	03/07/2025 41.33±0.04	04/07/2025 35.76±0.01	05/07/2025 33.71±0.03	06/07/2025 45.38±0.08
Nambekaha (Crop)	22/06/2024 37.62±0.02	23/06/2024 34.69±0.00	24/06/2024 34.61±0.00	25/06/2024 34.05±0.00	03/07/2025 41.72±0.02	04/07/2025 38.85±0.00	05/07/2025 38.20±0.01	06/07/2025 41.55±0.03
Lamto (Trees)	15/06/2024 38.11±0.00	16/06/2024 38.53±0.02	17/06/2024 39.18±0.00	18/06/2024 39.01±0.00	27/06/2025 37.65±0.00	28/06/2025 38.35±0.02	29/06/2025 39.44±0.00	30/06/2025 39.49±0.01
Lamto (Grass)	15/06/2024 30.48±0.00	16/06/2024 31.40±0.03	17/06/2024 31.06±0.00	18/06/2024 30.85±0.00	27/06/2025 45.18±0.03	28/06/2025 43.80±0.03	29/06/2025 38.35±0.01	30/06/2025 36.56±0.00
Lamto (Crop)	15/06/2024 25.73±1.35	16/06/2024 25.30±1.97	17/06/2024 24.31±1.50	18/06/2024 22.47±0.36	27/06/2025 33.47±1.29	28/06/2025 32.02±0.62	29/06/2025 30.78±0.21	30/06/2025 29.83±0.53
Dahra (Trees)	22/09/2024 17.60±0.00	23/09/2024 18.03±0.00	24/09/2024 25.09±0.05	25/09/2024 26.58±0.05	22/09/2025 17.42±0.00	23/09/2025 16.83±0.00	24/09/2025 16.64±0.00	25/09/2025 16.47±0.00
Dahra (Grass)	22/09/2024 17.60±0.00	23/09/2024 18.03±0.00	24/09/2024 25.09±0.05	25/09/2024 26.58±0.05	22/09/2025 14.75±0.00	23/09/2025 13.85±0.00	24/09/2025 12.85±0.00	25/09/2025 12.06±0.00
Dahra (Crop)					22/09/2025 23.02±0.00	23/09/2025 22.52±0.00	24/09/2025 21.91±0.00	25/09/2025 21.59±0.00

865 Table B2: interannual comparison (2024–2025) of soil moisture in the different ecosystems of each study site. Means correspond to the average of values measured during all the days of experiment.

Sites	Ecosystems	Years	t-student-statistic	p	p.signif	Years	Averages
Dahra	Grass	2024-2025	2.12502684	0.122	Not Significant	2024	21.83±4.67
						2025	16.84±0.41
Dahra	Trees	2024-2025	3.50652588	0.0326	*	2024	21.83±4.67
						2025	13.38±1.17
Lamto	Crops	2024-2025	-6.6054454	0.000596	***	2024	24.45±1.45
						2025	31.53±1.58
	Grass	2024-2025	-0.0492207	0.963	Not significant	2024	38.71±0.48
						2025	38.73±0.89
Trees	2024-2025	-4.7932799	0.0166	*	2024	30.95±0.39	
					2025	40.97±4.17	
Nambekaha	Crops	2024-2025	-2.5091883	0.0773	Not significant	2024	30.92±7.08
						2025	40.08±1.82
	Grass	2024-2025	1.43002936	0.204	Not significant	2024	28.66±3.11
						2025	25.73±2.66
Trees	2024-2025	-2.9971401	0.0386	*	2024	30.35±2.34	
					2025	39.05±5.31	



Appendix C: Variability of CO₂, CH₄, N₂O, and NO fluxes

Table C1: Average CO₂ fluxes (μg C m⁻² s⁻¹) in 2024 and 2025 for the four treatments on the three sites x three ecosystems

Sites (ecosystems)	Average CO ₂ (μg C m ⁻² s ⁻¹) flux 2024				Average CO ₂ (μg C m ⁻² s ⁻¹) flux 2025			
	Control C	Treatment S ₁	Treatment S ₂	Treatment S ₃	Control C	Treatment S ₁	Treatment S ₂	Treatment S ₃
Nambekaha (Trees)	50.63±9.1	49.46±10.0	51.59±7.9	52.09±15.8	74.00±40.8	50.94±7.7	41.27±6.1	47.67±15.7
Nambekaha (Grass)	44.05±12.7	41.24±10.4	52.12±5.5	54.51±22.9	50.01±6.9	42.75±8.5	51.42±24.2	60.54±21.3
Nambekaha (Crop)	24.26±8.0	16.87±3.6	15.74±4.9	21.37±9.0	39.81±19.7	37.08±1.9	43.98±17.7	46.47±16.1
Lamto (Trees)	42.56±9.9	37.44±6.2	34.91±5.5	39.37±4.2	45.53±21.6	45.72±19.5	35.74±9.1	91.35±73.2
Lamto (Grass)	34.42±4.2	29.82±4.2	33.58±8.4	46.58±8.5	49.23±23.8	47.57±10.7	36.88±19.8	45.50±26.2
Lamto (Crop)	47.82±2.3	58.96±5.4	58.21±29.7	67.98±30.2	61.33±15.9	41.19±2.6	47.08±6.0	59.85±2.3
Dahra (Trees)	19.57±11.7	20.82±6.2	21.60±4.4	22.48±5.3	51.84±8.5	64.75±11.1	55.44±11.2	59.29±4.0
Dahra (Grass)	26.71±3.0	14.10±8.0	24.90±5.7	24.59±1.3	52.59±8.1	55.95±6.6	58.29±8.8	64.49±16.3
Dahra (Crop)	8.21±2.5	18.75±12.7	10.50±4.8	12.92±2.2	27.39±7.7	33.26±8.1	34.36±7.2	33.14±9.7
	Average CO ₂ (μg C m ⁻² s ⁻¹) flux treatments 2024				Average CO ₂ (μg C m ⁻² s ⁻¹) flux treatments 2025			
Nambekaha (Trees)	50.94±11.8				53.47±25.6			
Nambekaha (Grass)	47.98±15.4				51.18±18.1			
Nambekaha (Crop)	19.56±7.6				41.83±15.9			
Lamto (Trees)	38.57±7.3				54.59±45.1			
Lamto (Grass)	36.10±9.2				44.80±21.5			
Lamto (Crop)	58.24±22.5				52.36±12.1			
Dahra (Trees)	21.12±7.5				57.83±10.4			
Dahra (Grass)	22.58±7.2				56.93±12.0			
Dahra (Crop)	12.59±8.0				32.04±8.7			

875 Table C2: Average CH₄ fluxes (ng C m⁻² s⁻¹) in 2024 and 2025 for the four treatments on the three sites x three ecosystems

Sites (ecosystems)	Average CH ₄ (ng C m ⁻² s ⁻¹) flux 2024				Average CH ₄ (ng C m ⁻² s ⁻¹) flux 2025			
	Control C	Treatment S ₁	Treatment S ₂	Treatment S ₃	Control C	Treatment S ₁	Treatment S ₂	Treatment S ₃
Nambekaha (Trees)	1.43±5.6	-2.23±1.3	4.86±7.5	-0.64±3.6	2.95±5.5	1.91±3.6	0.00±2.1	-2.23±1.0
Nambekaha (Grass)	3.42±4.3	5.41±5.3	3.26±2.9	10.35±12.5	3.50±1.5	1.75±1.0	11.78±12.2	4.38±5.6
Nambekaha (Crop)	-1.75±0.4	-1.27±0.2	-1.45±1.2	-1.19±0.1	-2.07±0.4	-2.47±1.2	-3.03±0.9	-2.39±1.4
Lamto (Trees)	-0.96±1.4	-1.43±0.4	-1.43±0.7	-2.15±0.6	-1.19±0.5	-1.43±1.6	-2.71±3.3	-0.08±7.4
Lamto (Grass)	-1.49±0.8	-0.24±1.6	-0.32±0.0	-1.11±1.0	0.32±2.4	2.97±3.0	2.44±3.4	0.56±1.7
Lamto (Crop)	-2.15±2.1	-2.47±1.7	-0.32±1.8	-5.02±2.0	-3.26±0.7	-4.38±1.3	-3.40±1.1	-4.94±1.9
Dahra (Trees)	0.00±1.5	1.11±0.5	0.34±1.5	1.06±0.4	0.08±1.1	0.00±1.5	-0.16±1.5	0.08±1.5
Dahra (Grass)	-0.08±1.6	1.03±0.3	0.16±1.0	1.59±1.5	-1.11±1.4	-1.35±0.5	-2.23±0.7	-1.67±1.4
Dahra (Crop)	-0.72±2.4	-3.08±1.0	-0.64±2.6	-0.40±1.4	0.08±1.2	0.56±1.5	0.80±0.9	0.64±1.5
	Average CH ₄ (ng C m ⁻² s ⁻¹) flux treatments 2024				Average CH ₄ (ng C m ⁻² s ⁻¹) flux treatments 2025			
Nambekaha (Trees)	0.86±5.7				0.66±4.0			
Nambekaha (Grass)	5.61±7.8				5.35±7.8			
Nambekaha (Crop)	-1.42±0.7				-2.49±1.1			



Lamto (Trees)	-1.53±0.9	-1.35±4.2
Lamto (Grass)	-0.85±1.3	1.49±2.9
Lamto (Crop)	-2.49±2.5	-4.03±1.5
Dahra (Trees)	0.60±1.2	0±1.4
Dahra (Grass)	0.68±1.4	-1.59±1.2
Dahra (Crop)	-1.08±2.2	0.52±1.3

Table C3: Average N₂O fluxes (ng N m⁻² s⁻¹) 2024 and 2025 for the four treatments on the three sites x three ecosystems

Sites (ecosystems)	Averages N ₂ O (ng N m ⁻² s ⁻¹) flux 2024				Averages N ₂ O (ng N m ⁻² s ⁻¹) flux 2025			
	Control C	Treatment S ₁	Treatment S ₂	Treatment S ₃	Control C	Treatment S ₁	Treatment S ₂	Treatment S ₃
Nambekaha (Trees)	2.23±7.4	-8.92±0.0	-3.72±0.0	-7.43±1.8	-2.79±5.3	-5.57±0.4	-3.72±0.0	-6.44±2.9
Nambekaha (Grass)	7.43±0.0	-0.99±4.4	1.11±6.3	-4.46±5.0	-5.20±1.8	2.23±6.7	-2.72±6.5	-6.44±0.9
Nambekaha (Crop)	27.12±8.5	6.44±1.9	9.29±4.7	22.66±25.1	-11.52±7.1	3.96±5.99	-2.97±6.1	2.23±3.8
Lamto (Trees)	-12.26±6.3	-4.83±0.4	-11.39±4.9	-14.86±4.5	-14.00±0.0	-7.99±9.5	5.70±13.3	-7.99±1.4
Lamto (Grass)	-10.40±3.7	-14.37±6.4	-6.32±1.1	-18.33±6.7	0.74±8.9	-2.60±4.8	-8.55±11.7	-13.62±7.2
Lamto (Crop)	10.40±0.0	5.57±0.4	4.46±6.6	3.22±10.2	-17.28±5.3	-12.63±7.4	-10.40±6.3	-4.64±10.6
Dahra (Trees)	2.23±11.9	4.95±17.9	12.63±20.0	-14.12±0.0	0.74±8.4	0.19±7.6	-8.92±6.3	-1.11±3.7
Dahra (Grass)	-5.94±0.0	-16.59±8.3	-10.77±1.1	-18.58±0.0	-8.17±4.4	-5.57±3.2	-5.94±2.6	-1.73±2.9
Dahra (Crop)		-11.89±0.0			-8.67±0.9	1.86±5.6	-5.39±6.2	-0.56±11.6
	Average N ₂ O (ng N m ⁻² s ⁻¹) flux treatments 2024				Average N ₂ O (ng N m ⁻² s ⁻¹) flux treatments 2025			
Nambekaha (Trees)		-4.35±6.1				-4.53±4.0		
Nambekaha (Grass)		-1.11±6.0				-3.51±5.5		
Nambekaha (Crop)		15.49±16.7				-1.36±7.8		
Lamto (Trees)		-10.90±5.8				-5.08±10.8		
Lamto (Grass)		-13.15±6.9				-6.50±10.6		
Lamto (Crop)		4.90±7.3				-11.10±9.3		
Dahra (Trees)		1.82±17.7				-2.48±7.7		
Dahra (Grass)		-13.69±6.9				-5.60±4.0		
Dahra (Crop)		-8.55±3.3				-2.82±8.4		

880 Table C4: Average NO fluxes (ng N m⁻² s⁻¹) in 2024 and 2025 for the four treatments on the three sites x three ecosystems

Sites (ecosystems)	Averages NO (ng N m ⁻² s ⁻¹) flux 2024				Averages (ng N m ⁻² s ⁻¹) flux 2025			
	Control C	Treatment S ₁	Treatment S ₂	Treatment S ₃	Control C	Treatment S ₁	Treatment S ₂	Treatment S ₃
Nambekaha (Trees)	26.01±10.7	11.01±6.0	9.98±6.3	7.74±2.7	0.62±0.2	0.58±0.1	0.78±0.3	0.62±0.5
Nambekaha (Grass)	10.18±4.7	11.26±4.0	20.24±5.0	39.92±22.0	0.34±0.1	0.36±0.1	0.45±0.2	0.35±0.2
Nambekaha (Crop)	497.39±14.6.3	402.12±28.3.2	383.88±74.0	348.44±68.9	2.92±0.8	1.94±1.2	2.38±0.5	2.45±1.1
Lamto (Trees)	0.01±0.0	0.08±0.1	0.04±0.0	0.09±0.1	0.55±0.7	0.11±0.1	0.11±0.0	0.25±0.3
Lamto (Grass)	0.05±0.0	0.01±0.0	0.02±0.0	0.09±0.1	1.68±1.4	0.64±0.3	1.33±1.1	0.67±0.5
Lamto (Crop)	0.37±0.4	0.23±0.2	0.09±0.0	0.13±0.1	1.18±0.7	1.47±0.7	0.71±0.3	1.01±0.3
Dahra (Trees)					0.58±0.3	1.27±1.6	0.68±0.4	0.54±0.2



Dahra (Grass)	0.42±0.0	0.34±0.1	0.44±0.1	0.44±0.0
Dahra (Crop)	3.30±0.6	2.96±0.5	3.37±0.3	2.89±0.8
Average NO (ng N m ⁻² s ⁻¹) flux treatments 2024		Average NO (ng N m ⁻² s ⁻¹) flux treatments 2025		
Nambekaha (Trees)	13.68±10.1	0.65±0.3		
Nambekaha (Grass)	20.40±16.7	0.37±0.2		
Nambekaha (Crop)	411.92±180.3	2.42±1.01		
Lamto (Trees)	0.06±0.1	0.27±0.4		
Lamto (Grass)	0.04±0.1	1.08±1.0		
Lamto (Crop)	0.19±0.2	1.09±0.6		
Dahra (Trees)		0.77±0.9		
Dahra (Grass)		0.41±0.1		
Dahra (Crop)		3.14±0.6		

885

890

895

900



Data availability

The datasets generated and analysed during this study are publicly available in the Zenodo repository: <https://doi.org/10.5281/zenodo.21128558>. The repository contains the raw and processed datasets, metadata, and R scripts used in this study

Author contributions

MZ participated in the field campaigns, processed and analysed the data, performed the statistical analyses, prepared the figures, and wrote the original manuscript. The study was conceptualized and designed by CD, DS, CGL, XLR and SB. CD participated in the field campaigns, supervised the research, the processing and the analyze of data, and revised the manuscript. SB participated in the fields campaigns, contributed to the statistical analysis, data analysis, interpretation of results, and critical revision of manuscript. DS and CGL participated in the field campaigns, discussed the results and revised the manuscript. AD participated in the field campaigns and revised the manuscript. MO, FK, SMB, AD, SS, ON, SK, ND participated in the fields campaigns. OL, MDA and EG analyzed the chemical samples. FS and HVD revised the manuscript. All authors contributed to the final version of the manuscript, and approved its submission.

Competing interests

The authors declare that they have no conflict of interest.

Acknowledgements

The authors would like to thank Demba Ba, Pathé Lo, and Nogmana Soumaguel for their valuable assistance during the field campaigns and data collection at Dahra. We are also grateful to Sana Yéo and Youssouf Doumbia for their support during field activities in Korhogo. At Lamto, we sincerely thank Ismaël Konaté, Adja Ki, Anzoumana Ouattara, and Thierry Henri Des Tureaux for their help during field measurements. Their contributions were essential to the successful completion of this study.

Financial support

This research was supported by the NitroAfrica project (ANR-22-CE01-0022) funded by the French Agence Nationale de la Recherche (ANR).

930

935



References

- Abbadie, L., Gignoux, J., Le Roux, X., and Lepage, M. (Eds.). (2006). *Lamto : Structure, Functioning, and Dynamics of a Savanna Ecosystem* (Vol. 179). Springer New York. <https://doi.org/10.1007/0-387-33857-8>
- 940 Abdalla, K., Chivenge, P., Ciais, P., and Chaplot, V. (2016). No-tillage lessens soil CO₂ emissions the most under arid and sandy soil conditions : Results from a meta-analysis. *Biogeosciences*, *13*(12), 3619-3633. <https://doi.org/10.5194/bg-13-3619-2016>
- Agbohessou, Y., Delon, C., Grippa, M., Mougin, E., Ngom, D., Gaglo, E. K., Ndiaye, O., Salgado, P., and Roupsard, O. (2024). Modelling CO₂ and N₂O emissions from soils in silvopastoral systems of the West African Sahelian band. *Biogeosciences*, *21*(11), 2811-2837. <https://doi.org/10.5194/bg-21-2811-2024>
- 945 Assouma, M. H., Serça, D., Guérin, F., Blanfort, V., Lecomte, P., Touré, I., Ickowicz, A., Manlay, R. J., Bernoux, M., and Vayssières, J. (2017). Livestock induces strong spatial heterogeneity of soil CO₂, N₂O and CH₄ emissions within a semi-arid sylvo-pastoral landscape in West Africa. *Journal of Arid Land*, *9*(2), 210-221. <https://doi.org/10.1007/s40333-017-0001-y>
- 950 Ba, S. M., Roupsard, O., Chapuis-Lardy, L., Bouvery, F., Agbohessou, Y., Duthoit, M., Wieckowski, A., Tagesson, T., Assouma, M. H., Gaglo, E. K., Delon, C., Sambou, B., and Serça, D. (2026). Drivers and vertical CO₂ flux balances in a Sahelian agroforestry system: Insights from high frequency measurements. *SOIL*, *12*(1), 471-495. <https://doi.org/10.5194/soil-12-471-2026>
- 955 Bateman, E. J., and Baggs, E. M. (2005). Contributions of nitrification and denitrification to N₂O emissions from soils at different water-filled pore space. *Biology and Fertility of Soils*, *41*(6), 379-388. <https://doi.org/10.1007/s00374-005-0858-3>
- 960 Bouwman, A. F., Boumans, L. J. M., and Batjes, N. H. (2002). Emissions of N₂O and NO from fertilized fields : Summary of available measurement data. *Global Biogeochemical Cycles*, *16*(4). <https://doi.org/10.1029/2001GB001811>
- Bratti, F., Luiz Locatelli, J., Henrique Ribeiro, R., Renan Besen, M., Dieckow, J., Bayer, C., and Thiago Piva, J. (2022). Nitrous oxide and methane emissions affected by grazing and nitrogen fertilization in an integrated crop-livestock system. *Geoderma*, *425*, 116027. <https://doi.org/10.1016/j.geoderma.2022.116027>
- 965 Butterbach-Bahl, K., Baggs, E. M., Dannenmann, M., Kiese, R., and Zechmeister-Boltenstern, S. (2013). Nitrous oxide emissions from soils : How well do we understand the processes and their controls? *Philosophical Transactions of the Royal Society B: Biological Sciences*, *368*(1621), 20130122. <https://doi.org/10.1098/rstb.2013.0122>
- 970 Cen, X., Müller, C., Kang, X., Zhou, X., Zhang, J., Yu, G., and He, N. (2024). Nitrogen deposition contributed to a global increase in nitrous oxide emissions from forest soils. *Communications Earth and Environment*, *5*(1), 532. <https://doi.org/10.1038/s43247-024-01647-6>
- 975 Chapuis-Lardy, L., Wrage, N., Metay, A., Chotte, J., and Bernoux, M. (2007). Soils, a sink for N₂O? A review. *Global Change Biology*, *13*(1), 1-17. <https://doi.org/10.1111/j.1365-2486.2006.01280.x>
- Clough, T. J., Sherlock, R. R., and Rolston, D. E. (2005). A Review of the Movement and Fate of N₂O in the Subsoil. *Nutrient Cycling in Agroecosystems*, *72*(1), 3-11. <https://doi.org/10.1007/s10705-004-7349-z>
- 980 Daelman, R., Bauters, M., Barthel, M., Bulonza, E., Lefevre, L., Mbifo, J., Six, J., Butterbach-Bahl, K., Wolf, B., Kiese, R., and Boeckx, P. (2025). Spatiotemporal variability of CO₂, N₂O and CH₄ fluxes from a semi-deciduous tropical forest soil in the Congo Basin. *Biogeosciences*, *22*(6), 1529-1542. <https://doi.org/10.5194/bg-22-1529-2025>



- 985 Davidson, E. A., and Verchot, L. V. (2000). Testing the Hole-in-the-Pipe Model of nitric and nitrous oxide emissions from soils using the TRAGNET Database. *Global Biogeochemical Cycles*, 14(4), 1035-1043. <https://doi.org/10.1029/1999GB001223>
- Delon, C., Galy-Lacaux, C., Barret, B., Ndiaye, O., Serça, D., Guérin, F., Gardrat, E., Mougin, E., Agbohessou, Y. F., and Probst, A. (2022). Nitrogen budget and critical load determination at a Sahelian grazed grassland site. *Nutrient Cycling in Agroecosystems*, 124(1), 17-34. <https://doi.org/10.1007/s10705-022-10220-6>
- 990 Delon, C., Galy-Lacaux, C., Boone, A., Liousse, C., Serça, D., Adon, M., Diop, B., Akpo, A., Lavenu, F., Mougin, E., and Timouk, F. (2010). Atmospheric nitrogen budget in Sahelian dry savannas. *Atmospheric Chemistry and Physics*, 10(6), 2691-2708. <https://doi.org/10.5194/acp-10-2691-2010>
- 995 Delon, C., Galy-Lacaux, C., Serça, D., Loubet, B., Camara, N., Gardrat, E., Saneh, I., Fensholt, R., Tagesson, T., Le Dantec, V., Sambou, B., Diop, C., and Mougin, E. (2017). Soil and vegetation-atmosphere exchange of NO, NH₃, and N₂O from field measurements in a semi arid grazed ecosystem in Senegal. *Atmospheric Environment*, 156, 36-51. <https://doi.org/10.1016/j.atmosenv.2017.02.024>
- 1000 Diawara, A., Yoroba, F., Kouadio, K. Y., Kouassi, K. B., Assamoi, E. M., Diedhiou, A., and Assamoi, P. (2014). Climate Variability in the Sudano-Guinean Transition Area and Its Impact on Vegetation : The Case of the Lamto Region in Côte D'Ivoire. *Advances in Meteorology*, 2014, 1-11. <https://doi.org/10.1155/2014/831414>
- 1005 Dijkstra, F. A., Morgan, J. A., Follett, R. F., and LeCain, D. R. (2013). Climate change reduces the net sink of CH₄ and N₂O in a semiarid grassland. *Global Change Biology*, 19(6), 1816-1826. <https://doi.org/10.1111/gcb.12182>
- Dlamini, J. C., Tesfamariam, E. H., Verbeeck, M., Loick, N., Louro-Lopez, A., Hawkins, J. M. B., Blackwell, M. S. A., Dunn, R. M., Collins, A. L., and Cardenas, L. M. (2024). Do NO, N₂O, N₂ and CO₂ fluxes differ in soils sourced from cropland and varying riparian buffer vegetation? An incubation study. *Soil Use and Management*, 40(1), e12951. <https://doi.org/10.1111/sum.12951>
- 1010 Duthoit, M., Roupsard, O., Créquy, N., and Sauze, J. (2020). *Le Cahier des Techniques de l'Inra 2020 (102)*.
- 1015 Fadnavis, S., Elshorbany, Y., Ziemke, J., Barret, B., Rap, A., Chandran, P. R. S., Pope, R. J., Sagar, V., Taraborrelli, D., Le Flochmoen, E., Cuesta, J., Wespes, C., Boersma, F., Glissenaar, I., De Smedt, I., Van Roozendaal, M., Petetin, H., and Anglou, I. (2025). Influence of nitrogen oxides and volatile organic compounds emission changes on tropospheric ozone variability, trends and radiative effect. *Atmospheric Chemistry and Physics*, 25(14), 8229-8254. <https://doi.org/10.5194/acp-25-8229-2025>
- 1020 Gallarotti, N., Barthel, M., Verhoeven, E., Pereira, E. I. P., Bauters, M., Baumgartner, S., Drake, T. W., Boeckx, P., Mohn, J., Longepierre, M., Mugula, J. K., Makelele, I. A., Ntaboba, L. C., and Six, J. (2021). In-depth analysis of N₂O fluxes in tropical forest soils of the Congo Basin combining isotope and functional gene analysis. *The ISME Journal*, 15(11), 3357-3374. <https://doi.org/10.1038/s41396-021-01004-x>
- 1025 Gong, C., Wang, Y., Tian, H., Kou-Giesbrecht, S., Vuichard, N., and Zaehle, S. (2025). Uncertainties in fertilizer-induced emissions of soil nitrogen oxide and the associated impacts on ground-level ozone and methane. *Atmospheric Chemistry and Physics*, 25(22), 17009-17025. <https://doi.org/10.5194/acp-25-17009-2025>
- 1030 Groffman, P. M., Butterbach-Bahl, K., Fulweiler, R. W., Gold, A. J., Morse, J. L., Stander, E. K., Tague, C., Tonitto, C., and Vidon, P. (2009). Challenges to incorporating spatially and temporally explicit phenomena (hotspots and hot moments) in denitrification models. *Biogeochemistry*, 93(1-2), 49-77. <https://doi.org/10.1007/s10533-008-9277-5>



- 1035 Kassamba-Diaby, M. L., Galy-Lacaux, C., Yoboué, V., Hickman, J. E., Mouchel-Vallon, C., Jaars, K., Gnamien, S., Konan, R., Gardrat, E., and Silué, S. (2023). The Chemical Characteristics of Rainwater and Wet Atmospheric Deposition Fluxes at Two Urban Sites and One Rural Site in Côte d'Ivoire. *Atmosphere*, 14(5), 809. <https://doi.org/10.3390/atmos14050809>
- 1040 Koffi, K. F., N'Dri, A. B., Lata, J.-C., Konaté, S., Srikanthasamy, T., Konan, M., and Barot, S. (2019). Effect of fire regime on the grass community of the humid savanna of Lamto, Ivory Coast. *Journal of Tropical Ecology*, 35(1), 1-7. <https://doi.org/10.1017/S0266467418000391>
- 1045 Konan, L. N., Koné, A. W., and Yao-Kouamé, A. (2021). *Stockage de carbone dans le sol sous les principaux arbustes en savane humide de Côte d'Ivoire (Lamto)*. <https://doi.org/10.13140/RG.2.2.36060.51843/1>
- Krichels, A. H., Homyak, P. M., Aronson, E. L., Sickman, J. O., Botthoff, J., Shulman, H., Piper, S., Andrews, H. M., and Jenerette, G. D. (2022). Rapid nitrate reduction produces pulsed NO and N₂O emissions following wetting of dryland soils. *Biogeochemistry*, 158(2), 233-250. <https://doi.org/10.1007/s10533-022-00896-x>
- 1050 Lamarque, J.-F., Dentener, F., McConnell, J., Ro, C.-U., Shaw, M., Vet, R., Bergmann, D., Cameron-Smith, P., Dalsoren, S., Doherty, R., Faluvegi, G., Ghan, S. J., Josse, B., Lee, Y. H., MacKenzie, I. A., Plummer, D., Shindell, D. T., Skeie, R. B., Stevenson, D. S., ... Nolan, M. (2013). Multi-model mean nitrogen and sulfur deposition from the Atmospheric Chemistry and Climate Model Intercomparison Project (ACCMIP): Evaluation of historical and projected future changes. *Atmospheric Chemistry and Physics*, 13(16), 7997-8018. <https://doi.org/10.5194/acp-13-7997-2013>
- 1055 Laouali, D., Delon, C., Adon, M., Ndiaye, O., Saneh, I., Gardrat, E., Dias-Alves, M., Tagesson, T., Fensholt, R., and Galy-Lacaux, C. (2021). Source contributions in precipitation chemistry and analysis of atmospheric nitrogen deposition in a Sahelian dry savanna site in West Africa. *Atmospheric Research*, 251, 105423. <https://doi.org/10.1016/j.atmosres.2020.105423>
- 1060 Le Mer, J., and Roger, P. (2001). Production, oxidation, emission and consumption of methane by soils : A review. *European Journal of Soil Biology*, 37(1), 25-50. [https://doi.org/10.1016/S1164-5563\(01\)01067-6](https://doi.org/10.1016/S1164-5563(01)01067-6)
- 1065 Leitner, S., Homyak, P. M., Blankinship, J. C., Eberwein, J., Jenerette, G. D., Zechmeister-Boltenstern, S., and Schimel, J. P. (2017). Linking NO and N₂O emission pulses with the mobilization of mineral and organic N upon rewetting dry soils. *Soil Biology and Biochemistry*, 115, 461-466. <https://doi.org/10.1016/j.soilbio.2017.09.005>
- 1070 Leitner, S. M., Carbonell, V., Mhindu, R. L., Zhu, Y., Mutuo, P., Butterbach-Bahl, K., and Merbold, L. (2024). Greenhouse gas emissions from cattle enclosures in semi-arid sub-Saharan Africa: The case of a rangeland in South-Central Kenya. *Agriculture, Ecosystems and Environment*, 367, 108980. <https://doi.org/10.1016/j.agee.2024.108980>
- 1075 Lim, J., Wehmeyer, H., Heffner, T., Aeppli, M., Gu, W., Kim, P. J., Horn, M. A., and Ho, A. (2024). Resilience of aerobic methanotrophs in soils; spotlight on the methane sink under agriculture. *FEMS Microbiology Ecology*, 100(3), fiae008. <https://doi.org/10.1093/femsec/fiae008>
- Linn, D. M., and Doran, J. W. (1984). Effect of Water-Filled Pore Space on Carbon Dioxide and Nitrous Oxide Production in Tilled and Nontilled Soils. *Soil Science Society of America Journal*, 48(6), 1267-1272. <https://doi.org/10.2136/sssaj1984.03615995004800060013x>
- 1080 Liu, H., Li, Y., Pan, B., Zheng, X., Yu, J., Ding, H., and Zhang, Y. (2022). Pathways of soil N₂O uptake, consumption, and its driving factors : A review. *Environmental Science and Pollution Research*, 29(21), 30850-30864. <https://doi.org/10.1007/s11356-022-18619-y>



- 1085 Liu, H., Zheng, X., Li, Y., Yu, J., Ding, H., Sveen, T. R., and Zhang, Y. (2022). Soil moisture determines nitrous oxide emission and uptake. *Science of The Total Environment*, 822, 153566. <https://doi.org/10.1016/j.scitotenv.2022.153566>
- 1090 Liu, Y., Ding, C., Xu, X., Wang, K., Li, Y., Pan, H., Zhang, Q., Dumont, M. G., Di, H., Xu, J., and Li, Y. (2022). Atmospheric methane oxidation is affected by grassland type and grazing and negatively correlated to total soil respiration in arid and semiarid grasslands in Inner Mongolia. *Soil Biology and Biochemistry*, 173, 108787. <https://doi.org/10.1016/j.soilbio.2022.108787>
- 1095 Lu, C., Yu, Z., Zhang, J., Cao, P., Tian, H., and Nevison, C. (2022). Century-long changes and drivers of soil nitrous oxide (N₂O) emissions across the contiguous United States. *Global Change Biology*, 28(7), 2505-2524. <https://doi.org/10.1111/gcb.16061>
- 1100 Ludwig, J., Meixner, F. X., Vogel, B., and Förstner, J. (2001). Soil-air exchange of nitric oxide : An overview of processes, environmental factors, and modeling studies. *Biogeochemistry*, 52(3), 225-257. <https://doi.org/10.1023/A:1006424330555>
- 1105 Matson, P. A., McDowell, W. H., Townsend, A. R., and Vitousek, P. M. (1999). The globalization of N deposition : Ecosystem consequences in tropical environments. *Biogeochemistry*, 46(1-3), 67-83. <https://doi.org/10.1007/BF01007574>
- 1110 Mieke, S., Kluge, J., Von Wehrden, H., and Retzer, V. (2010). Long-term degradation of Sahelian rangeland detected by 27 years of field study in Senegal : Long-term rangeland monitoring in the Sahel. *Journal of Applied Ecology*, 47(3), 692-700. <https://doi.org/10.1111/j.1365-2664.2010.01815.x>
- 1115 Moyano, F. E., Manzoni, S., and Chenu, C. (2013). Responses of soil heterotrophic respiration to moisture availability : An exploration of processes and models. *Soil Biology and Biochemistry*, 59, 72-85. <https://doi.org/10.1016/j.soilbio.2013.01.002>
- 1120 Ossouhou, M., Galy-Lacaux, C., Yoboué, V., Adon, M., Delon, C., Gardrat, E., Konaté, I., Ki, A., and Zouzou, R. (2021). Long-term atmospheric inorganic nitrogen deposition in West African savanna over 16 year period (Lamto, Côte d'Ivoire). *Environmental Research Letters*, 16(1), 015004. <https://doi.org/10.1088/1748-9326/abd065>
- 1125 Otieno, D. O., K'Otuto, G. O., Maina, J. N., Kuzyakov, Y., and Onyango, J. C. (2010). Responses of ecosystem carbon dioxide fluxes to soil moisture fluctuations in a moist Kenyan savanna. *Journal of Tropical Ecology*, 26(6), 605-618. <https://doi.org/10.1017/S0266467410000416>
- 1130 Pape, L., Ammann, C., Nyfeler-Brunner, A., Spirig, C., Hens, K., and Meixner, F. X. (2009). An automated dynamic chamber system for surface exchange measurement of non-reactive and reactive trace gases of grassland ecosystems. *Biogeosciences*, 6(3), 405-429. <https://doi.org/10.5194/bg-6-405-2009>
- 1135 Parton, W., Silver, W. L., Burke, I. C., Grassens, L., Harmon, M. E., Currie, W. S., King, J. Y., Adair, E. C., Brandt, L. A., Hart, S. C., and Fasth, B. (2007). Global-Scale Similarities in Nitrogen Release Patterns During Long-Term Decomposition. *Science*, 315(5810), 361-364. <https://doi.org/10.1126/science.1134853>
- 1140 Potter, C. S., Matson, P. A., Vitousek, P. M., and Davidson, E. A. (1996). Process modeling of controls on nitrogen trace gas emissions from soils worldwide. *Journal of Geophysical Research: Atmospheres*, 101(D1), 1361-1377. <https://doi.org/10.1029/95JD02028>
- 1145 Rasmussen, C., Troch, P. A., Chorover, J., Brooks, P., Pelletier, J., and Huxman, T. E. (2011). An open system framework for integrating critical zone structure and function. *Biogeochemistry*, 102(1-3), 15-29. <https://doi.org/10.1007/s10533-010-9476-8>
- 1150 Ravishankara, A. R., Daniel, J. S., and Portmann, R. W. (2009). Nitrous Oxide (N₂O) : The Dominant Ozone-Depleting Substance Emitted in the 21st Century. *Science*, 326(5949), 123-125. <https://doi.org/10.1126/science.1176985>



- 1135 Reay, D. S., Davidson, E. A., Smith, K. A., Smith, P., Melillo, J. M., Dentener, F., and Crutzen, P. J. (2012). Global agriculture and nitrous oxide emissions. *Nature Climate Change*, 2(6), 410-416. <https://doi.org/10.1038/nclimate1458>
- 1140 Reichstein, M., Rey, A., Freibauer, A., Tenhunen, J., Valentini, R., Banza, J., Casals, P., Cheng, Y., Grünzweig, J. M., Irvine, J., Joffre, R., Law, B. E., Loustau, D., Miglietta, F., Oechel, W., Ourcival, J., Pereira, J. S., Peressotti, A., Ponti, F., ... Yakir, D. (2003). Modeling temporal and large-scale spatial variability of soil respiration from soil water availability, temperature and vegetation productivity indices. *Global Biogeochemical Cycles*, 17(4), 2003GB002035. <https://doi.org/10.1029/2003GB002035>
- 1145 Robertson, G. P., Paul, E. A., and Harwood, R. R. (2000). Greenhouse Gases in Intensive Agriculture: Contributions of Individual Gases to the Radiative Forcing of the Atmosphere. *Science*, 289(5486), 1922-1925. <https://doi.org/10.1126/science.289.5486.1922>
- Savage, K., Phillips, R., and Davidson, E. (2014). High temporal frequency measurements of greenhouse gas emissions from soils. *Biogeosciences*, 11(10), 2709-2720. <https://doi.org/10.5194/bg-11-2709-2014>
- 1150 Serca, D., Delmas, R., Jambert, C., and Labroue, L. (1994). Emissions of nitrogen oxides from equatorial rain forest in central Africa: Origin and regulation of NO emission from soils. *Tellus B: Chemical and Physical Meteorology*, 46(4), 243. <https://doi.org/10.3402/tellusb.v46i4.15795>
- 1155 Serça, D., Delmas, R., Le Roux, X., Parsons, D. A. B., Scholes, M. C., Abbadie, L., Lensi, R., Ronce, O., and Labroue, L. (1998). Comparison of nitrogen monoxide emissions from several African tropical ecosystems and influence of season and fire. *Global Biogeochemical Cycles*, 12(4), 637-651. <https://doi.org/10.1029/98GB02737>
- 1160 Song, H., Peng, C., Zhu, Q., Chen, Z., Blanchet, J.-P., Liu, Q., Li, T., Li, P., and Liu, Z. (2024). Quantification and uncertainty of global upland soil methane sinks: Processes, controls, model limitations, and improvements. *Earth-Science Reviews*, 252, 104758. <https://doi.org/10.1016/j.earscirev.2024.104758>
- 1165 Srikanthasamy, T., Leloup, J., N'Dri, A. B., Barot, S., Gervaix, J., Koné, A. W., Koffi, K. F., Le Roux, X., Raynaud, X., and Lata, J.-C. (2018). Contrasting effects of grasses and trees on microbial N-cycling in an African humid savanna. *Soil Biology and Biochemistry*, 117, 153-163. <https://doi.org/10.1016/j.soilbio.2017.11.016>
- 1170 Stehfest, E., and Bouwman, L. (2006). N₂O and NO emission from agricultural fields and soils under natural vegetation: Summarizing available measurement data and modeling of global annual emissions. *Nutrient Cycling in Agroecosystems*, 74(3), 207-228. <https://doi.org/10.1007/s10705-006-9000-7>
- 1175 Syakila, A., and Kroeze, C. (2011). The global nitrous oxide budget revisited. *Greenhouse Gas Measurement and Management*, 1(1), 17-26. <https://doi.org/10.3763/ghgmm.2010.0007>
- Tagesson, T., Fensholt, R., Cropley, F., Guiro, I., Horion, S., Ehammer, A., and Ardö, J. (2015). Dynamics in carbon exchange fluxes for a grazed semi-arid savanna ecosystem in West Africa. *Agriculture, Ecosystems and Environment*, 205, 15-24. <https://doi.org/10.1016/j.agee.2015.02.017>
- 1180 Tian, H., Xu, R., Canadell, J. G., Thompson, R. L., Winiwarter, W., Suntharalingam, P., Davidson, E. A., Ciais, P., Jackson, R. B., Janssens-Maenhout, G., Prather, M. J., Regnier, P., Pan, N., Pan, S., Peters, G. P., Shi, H., Tubiello, F. N., Zaehle, S., Zhou, F., ... Yao, Y. (2020). A comprehensive quantification of global nitrous oxide sources and sinks. *Nature*, 586(7828), 248-256. <https://doi.org/10.1038/s41586-020-2780-0>
- Tiemoko, D. T., Yoroba, F., Diawara, A., Kouadio, K., Kouassi, B. K., and Yapo, A. L. M. (2020). Understanding the Local Carbon Fluxes Variations and Their Relationship to Climate



- Conditions in a Sub-Humid Savannah-Ecosystem during 2008-2015 : Case of Lamto in Cote d'Ivoire. *Atmospheric and Climate Sciences*, 10(02), 186-205.
1185 <https://doi.org/10.4236/acs.2020.102010>
- Tiemoko, D. T., Yoroba, F., Kouassi, K. B., Diawara, A., Kouadio, K., Bouo, F.-X. D. B., Yapo, A. L. M., Kouman, A., and Ramonet, M. (2023). CO₂, CH₄, and CO Emission Sources and Their Characteristics in the Lamto Ecological Reserve (Côte d'Ivoire). *Atmosphere*, 14(10), 1533. <https://doi.org/10.3390/atmos14101533>
- 1190 Van Lent, J., Hergoualc'h, K., and Verchat, L. V. (2015). Reviews and syntheses : Soil N₂ O and NO emissions from land use and land-use change in the tropics and subtropics: a meta-analysis. *Biogeosciences*, 12(23), 7299-7313. <https://doi.org/10.5194/bg-12-7299-2015>
- 1195 Vet, R., Artz, R. S., Carou, S., Shaw, M., Ro, C.-U., Aas, W., Baker, A., Bowersox, V. C., Dentener, F., Galy-Lacaux, C., Hou, A., Pienaar, J. J., Gillett, R., Forti, M. C., Gromov, S., Hara, H., Khodzher, T., Mahowald, N. M., Nickovic, S., ... Reid, N. W. (2014). A global assessment of precipitation chemistry and deposition of sulfur, nitrogen, sea salt, base cations, organic acids, acidity and pH, and phosphorus. *Atmospheric Environment*, 93, 3-100. <https://doi.org/10.1016/j.atmosenv.2013.10.060>
- 1200 Wang, C., Amon, B., Schulz, K., and Mehdi, B. (2021). Factors That Influence Nitrous Oxide Emissions from Agricultural Soils as Well as Their Representation in Simulation Models : A Review. *Agronomy*, 11(4), 770. <https://doi.org/10.3390/agronomy11040770>
- 1205 Wang, W., Ciais, P., Nemani, R. R., Canadell, J. G., Piao, S., Sitch, S., White, M. A., Hashimoto, H., Milesi, C., and Myneni, R. B. (2013). Variations in atmospheric CO₂ growth rates coupled with tropical temperature. *Proceedings of the National Academy of Sciences*, 110(32), 13061-13066. <https://doi.org/10.1073/pnas.1219683110>
- 1210 Wieckowski, A., Vestin, P., Ardö, J., Roupsard, O., Ndiaye, O., Ba, S., Delon, C., Serça, D., and Tagesson, T. (2026). Contrasting roles of ground, trees, ponds and grazing in carbon dioxide, methane and nitrous oxide fluxes of an African semi-arid savanna. *Agriculture, Ecosystems and Environment*, 399, 110199. <https://doi.org/10.1016/j.agee.2025.110199>
- Wild, J., Kopecký, M., Macek, M., Šanda, M., Jankovec, J., and Haase, T. (2019). Climate at ecologically relevant scales : A new temperature and soil moisture logger for long-term microclimate measurement. *Agricultural and Forest Meteorology*, 268, 40-47. <https://doi.org/10.1016/j.agrformet.2018.12.018>
- 1215 Williams, E. J., and Davidson, E. A. (1993). An intercomparison of two chamber methods for the determination of emission of nitric oxide from soil. *Atmospheric Environment. Part A. General Topics*, 27(14), 2107-2113. [https://doi.org/10.1016/0960-1686\(93\)90040-6](https://doi.org/10.1016/0960-1686(93)90040-6)
- Wu, D., Dong, W., Oenema, O., Wang, Y., Trebs, I., and Hu, C. (2013). N₂O consumption by low-nitrogen soil and its regulation by water and oxygen. *Soil Biology and Biochemistry*, 60, 165-172. <https://doi.org/10.1016/j.soilbio.2013.01.028>
- 1220 Yagle, I., and Gelfand, I. (2025). Abiotic reactions drive post-wetting soil emissions of N₂O and NO and contribute partially to CO₂ emissions. *Scientific Reports*, 15(1), 27818. <https://doi.org/10.1038/s41598-025-12362-3>
- 1225 Zaman, M., Kleineidam, K., Bakken, L., Berendt, J., Bracken, C., Butterbach-Bahl, K., Cai, Z., Chang, S. X., Clough, T., Dawar, K., Ding, W. X., Dörsch, P., Dos Reis Martins, M., Eckhardt, C., Fiedler, S., Frosch, T., Goopy, J., Görres, C.-M., Gupta, A., ... Müller, C. (2021). Greenhouse Gases from Agriculture. In M. Zaman, L. Heng, and C. Müller (Eds.), *Measuring Emission of Agricultural Greenhouse Gases and Developing Mitigation Options using Nuclear and Related Techniques* (p. 1-10). Springer International Publishing. https://doi.org/10.1007/978-3-030-55396-8_1
- 1230 Zhang, Q., Li, Y., Wang, M., Wang, K., Meng, F., Liu, L., Zhao, Y., Ma, L., Zhu, Q., Xu, W., and Zhang, F. (2021). Atmospheric nitrogen deposition : A review of quantification

<https://doi.org/10.5194/egusphere-2026-3592>

Preprint. Discussion started: 6 July 2026

© Author(s) 2026. CC BY 4.0 License.



1235

methods and its spatial pattern derived from the global monitoring networks.

Ecotoxicology and Environmental Safety, 216, 112180.

<https://doi.org/10.1016/j.ecoenv.2021.112180>